

Supporting Information for:

Catalytic activation via π -backbonding in halogen bonds

Andrew Wang^{a,†} and Pierre Kennepohl^{a,c}

- a. Department of Chemistry, University of British Columbia, 2036 Main Mall, Vancouver, BC, Canada
- b. Department of Chemistry, University of Calgary, 2500 University Drive NW, Calgary, AB, Canada

† Current address: Department of Chemistry, University of Toronto, 80 St. George Street, Toronto, ON, Canada

ac.wang@mail.utoronto.ca

pierre.kennepohl@ucalgary.ca

Table of contents

1.	Computational methods.....	3
2.	Extended discussions.....	6
2.1	Extended discussion of NPA analysis.....	6
2.1.1	PF ₃	6
2.1.2	NH ₃	10
2.1.3	CO.....	12
2.2	More discussion on charge decomposition analysis	14
3.	Figures.....	16
3.1	$\Delta G_{\text{XB}}^{\ddagger}$ vs. $\Delta G_{\text{ref}}^{\ddagger}$ and ΔH_{XB}^0 vs. $E^{(2)}[\sigma^*]$	17
3.2	Changes in bond lengths and NPA charges for CO and NH ₃ as electron donors.....	19
3.3	NPA correlation plots.....	21
3.4	π -type MO figures for all sets of substituents (calculated at M06-2X/def2-TZVP)	27
3.4.1	PF ₃ and NH ₃	27
3.5	Gaussian-broadened TDOS for all sets of substituents	38
4.	Tables	39
4.1	Data for $\Delta H_{\text{XB}}^0[\text{GS}]$ and $\Delta H_{\text{XB}}^0[\text{TS}]$	39
4.2	Raw thermochemical data for GS and TS structures	40
4.3	Geometric and other data relevant for XB for GS and TS	43
4.4	NPA raw data.....	47
4.5	Expanded tables for CDA	49
5.	Cartesian coordinates and electronic energies of ground state and transition state structures.....	51
5.1	Ground state	51
5.1.1	Ground state, CO as electron donor	51
5.1.2	Ground state, PF ₃ as electron donor.....	54
5.1.3	Ground state, NH ₃ as electron donor	57
5.1.4	Ground state, no XB	60
5.2	Transition state.....	63
5.2.1	Transition state, CO as electron donor	63
5.2.2	Transition state, PF ₃ as electron donor.....	66
5.2.3	Transition state, NH ₃ as electron donor	69
5.2.4	Transition state, no XB	72
5.2.5	Transition state, PH ₃ as electron donor.....	75
5.3	Electron donors	78

1. Computational methods

Geometry optimization and thermochemistry: All calculations were performed using the Gaussian 09 software (G09)¹ with molecules built in WebMO.² The M06-2X functional³ was used for all calculations owing to its excellent performance on describing thermochemical kinetics and intermolecular interactions,^{3,4} and the aug-cc-pVDZ-PP basis set (parameters obtained from the ESLM basis set exchange^{5,6}) was used for iodine and jun-cc-pVDZ⁷ for all other elements. All calculations were performed in the gas phase, at 298.15 K, and 1 atm using an ultrafine integration grid (99 radial shells, 590 angular points).

Ground state structures were optimized to a minimum from a starting distance of ~3 Å between the donor and acceptor atoms and an initial XB angle of ~180 degrees, then followed by frequency calculations for the thermochemical data (calculated from the electronic energies (Section 4 of this document) according to ref. ⁸) and to verify the absence of imaginary frequencies.

Transition state calculations were first performed without XB, with an initial search for the transition state via a relaxed potential energy surface scan along the reaction coordinate (distance between the incoming iodide and the electrophilic carbon), then optimized with the Berny algorithm.^{9–13} The QST2 algorithm¹⁴ was used when the Berny algorithm fails to produce an accurate transition state structure. Frequency calculations are then carried out for the thermochemical data and to verify the presence of exactly one imaginary frequency with the vibrational mode corresponding to substitution of LG by Nu along the reaction coordinate. Transition state structures with XB were optimized from an initial configuration consisting of the optimized TS of the geminal iodide and the electron donor placed at a distance of ~ 3 Å between the donor and acceptor atoms and an initial XB angle of ~180 degrees, followed by the same procedure for optimizing the TS without XB.

Generalizing the XB stabilization energies in the GS and TS to being any thermodynamic quantity E (for this study $E = H$ or $E = G$), the XB stabilization (ΔE_{XB}) is calculated as follows:

$$\Delta E_{\text{XB}} = E_{\text{complex}} - (E_{\text{diiodomethane}} + E_{\text{electron donor}})$$

where $E_{\text{diiodomethane}}$ and $E_{\text{electron donor}}$ refer to the corresponding isolated species. Because of the nature of the square scheme involved in this study (Scheme 1), it follows from conservation of energy that

$$\Delta \Delta E^\ddagger = \Delta E_{\text{XB}}^\ddagger - \Delta E_{\text{ref}}^\ddagger = \Delta E_{\text{XB}}[\text{TS}] - \Delta E_{\text{XB}}[\text{GS}]$$

($E_{\text{electron donor}}$ cancels out in the derivation).

Single point calculations, MO analysis, TDOS, CDA, and NBO/NPA: Single point calculations were performed using G09 with both M06-2X/jun-cc-pVDZ (aug-cc-pVDZ-PP for iodine) and M06-2X/def2-TZVP. The results of MO analysis from the def2-TZVP and jun/aug-cc-pVDZ basis sets were qualitatively similar for the entire series of diiodomethanes, so the former was used for NBO calculations and density of states. For MO plotting (diagrams/figures) and CDA, M06-2X/def2-TZVP was used.

NBO and NPA calculations were carried out with the NBO package built into G09. MO energy diagrams, CDA, and Gaussian-broadened density of states (calculated via the Hirshfield method) were obtained using Multiwfn.¹⁵ MO cube files (~512 000 grid points) were generated using Multiwfn, rendered using the Visual Molecular Dynamics software,¹⁶ and traced with POV-Ray 3.6.¹⁷

References:

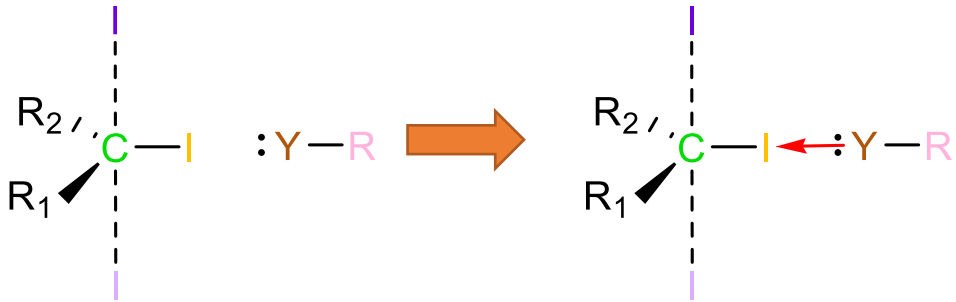
- (1) Gaussian 09, Revision D.01, M. J. Frisch, G. W. Trucks, H. B. Schlegel, G. E. Scuseria, M. A. Robb, J. R. Cheeseman, G. Scalmani, V. Barone, G. A. Petersson, H. Nakatsuji, X. Li, M. Caricato, A. Marenich, J. Bloino, B. G. Janesko, R. Gomperts, B. Mennucci, H. P. Hratchian, J. V. Ortiz, A. F. Izmaylov, J. L. Sonnenberg, D. Williams-Young, F. Ding, F. Lipparini, F. Egidi, J. Goings, B. Peng, A. Petrone, T. Henderson, D. Ranasinghe, V. G. Zakrzewski, J. Gao, N. Rega, G. Zheng, W. Liang, M. Hada, M. Ehara, K. Toyota, R. Fukuda, J. Hasegawa, M. Ishida, T. Nakajima, Y. Honda, O. Kitao, H. Nakai, T. Vreven, K. Throssell, J. A. Montgomery, Jr., J. E. Peralta, F. Ogliaro, M. Bearpark, J. J. Heyd, E. Brothers, K. N. Kudin, V. N. Staroverov, T. Keith, R. Kobayashi, J. Normand, K. Raghavachari, A. Rendell, J. C. Burant, S. S. Iyengar, J. Tomasi, M. Cossi, J. M. Millam, M. Klene, C. Adamo, R. Cammi, J. W. Ochterski, R. L. Martin, K. Morokuma, O. Farkas, J. B. Foresman, and D. J. Fox, *Gaussian, Inc.*, Wallingford CT, 2016.
- (2) Schmidt, J.R.; Polik, W.F. *WebMO Enterprise, Version 20.0*; WebMO LLC: Holland, MI, USA, 2020.
- (3) Zhao, Y.; Truhlar, D. G. The M06 Suite of Density Functionals for Main Group Thermochemistry, Thermochemical Kinetics, Noncovalent Interactions, Excited States, and Transition Elements: Two New Functionals and Systematic Testing of Four M06-Class Functionals and 12 Other Functionals. *Theor. Chem. Acc.* **2008**, 120 (1–3), 215–241. <https://doi.org/10.1007/s00214-007-0310-x>.
- (4) Cohen, A. J.; Mori-Sánchez, P.; Yang, W. Challenges for Density Functional Theory. *Chem. Rev.* **2012**, 112 (1), 289–320. <https://doi.org/10.1021/cr200107z>.
- (5) Feller, D. The Role of Databases in Support of Computational Chemistry Calculations. *J. Comput. Chem.* **1996**, 17 (13), 1571–1586.
- (6) Schuchardt, K. L.; Didier, B. T.; Elsethagen, T.; Sun, L.; Gurumoorthi, V.; Chase, J.; Li, J.; Windus, T. L. Basis Set Exchange: A Community Database for Computational Sciences. *J. Chem. Inf. Model.* **2007**, 47 (3), 1045–1052. <https://doi.org/10.1021/ci600510j>.

- (7) Papajak, E.; Zheng, J.; Xu, X.; Leverentz, H. R.; Truhlar, D. G. Perspectives on Basis Sets Beautiful: Seasonal Plantings of Diffuse Basis Functions. *J. Chem. Theory Comput.* **2011**, 7 (10), 3027–3034. <https://doi.org/10.1021/ct200106a>.
- (8) Ochterski, J. W. Thermochemistry in Gaussian. **2000**.
- (9) Bernhard Schlegel, H. Estimating the Hessian for Gradient-Type Geometry Optimizations. *Theor. Chim. Acta* **1984**, 66 (5), 333–340. <https://doi.org/10.1007/BF00554788>.
- (10) Simons, J.; Joergensen, P.; Taylor, H.; Ozment, J. Walking on Potential Energy Surfaces. *J. Phys. Chem.* **1983**, 87 (15), 2745–2753. <https://doi.org/10.1021/j100238a013>.
- (11) Banerjee, A.; Adams, N.; Simons, J.; Shepard, R. Search for Stationary Points on Surfaces. *J. Phys. Chem.* **1985**, 89 (1), 52–57. <https://doi.org/10.1021/j100247a015>.
- (12) Baker, J. An Algorithm for the Location of Transition States. *J. Comput. Chem.* **1986**, 7 (4), 385–395. <https://doi.org/10.1002/jcc.540070402>.
- (13) Baker, J. An Algorithm for Geometry Optimization without Analytical Gradients. *J. Comput. Chem.* **1987**, 8 (5), 563–574. <https://doi.org/10.1002/jcc.540080502>.
- (14) Peng, C.; Bernhard Schlegel, H. Combining Synchronous Transit and Quasi-Newton Methods to Find Transition States. *Isr. J. Chem.* **1993**, 33 (4), 449–454. <https://doi.org/10.1002/ijch.199300051>.
- (15) Lu, T.; Chen, F. Multiwfn: A Multifunctional Wavefunction Analyzer. *J. Comput. Chem.* **2012**, 33 (5), 580–592. <https://doi.org/10.1002/jcc.22885>.
- (16) Humphrey, W.; Dalke, A.; Schulten, K. VMD: Visual Molecular Dynamics. *J. Mol. Graph.* **1996**, 14 (1), 33–38. [https://doi.org/10.1016/0263-7855\(96\)00018-5](https://doi.org/10.1016/0263-7855(96)00018-5).
- (17) Persistence of Vision Pty. Ltd., Persistence of Vision Raytracer (Version 3.6), 2004, <http://www.povray.org/Download/>.

2. Extended discussions

2.1 Extended discussion of NPA analysis

We discuss the change in NPA charges (Δq) going from no XB to XB on the groups shown in Figure S4 (reproduced below), with Nu = the incoming iodide (dark purple), LG = the leaving iodide (light purple), C[E] = the electrophilic carbon (green), I[XB] = the iodine involved in XB (yellow), Y = the atom on the Lewis base directly involved in the XB interaction (brown; for PF_3 : Y = P, NH_3 : Y = N, CO: Y = C[=O]), Z = the remaining atoms on the Lewis base (pink; for PF_3 : Z = sum across the three fluorine atoms = 3F, NH_3 : Z = sum across the three hydrogen atoms = 3H, CO: Z = O).



2.1.1 PF_3

When PF_3 is the electron donor, we observe that $\Delta q > 0$ (i.e. decrease in electron density) on Nu, LG, and the phosphorus atom of PF_3 (P; i.e. Y = P). For I[XB], C[E], and the 3 fluorine atoms on PF_3 (3F; i.e. Z = 3F), $\Delta q < 0$ (i.e. there is an increase in electron density). The loss of electron density on Nu and LG are consistent with the decrease in bond lengths between each group and C[E] (Figure S5). The loss of electron density on P could imply charge transfer from P to the diiodomethane via a traditional σ -type pathway for XB, however we found no correlation between the changes in NPA charges on P, I[XB], and other groups. This can suggest that even though σ -donation is present, it is not well-defined. On the other hand, we found that the sum of Δq on the groups with $\Delta q > 0$ correlates with that for those with $\Delta q < 0$ (Figure S6a). Decomposition of that plot to examine Δq between individual atoms (Figure S8) suggests that electron density flows away from Nu and LG and shifts towards C[E], I[XB], and 3F. The direction of electron flow

is from the diiodomethane TS to PF_3 , and is indicative of a backbonding interaction from a standpoint where the commonly known XB interaction would be σ -donation of electron density from PF_3 to the diiodomethane. While σ -donation still exists in the XB interaction, (i.e. $\Delta q > 0$ for the sum of all PF_3 atoms (Figure S6b), which indicates that there is still forward σ -donation from PF_3 to the diiodomethane), we discuss below and demonstrate in Figure S7 that it is not important towards $\Delta H_{\text{XB}}^0[\text{TS}]$ and that π -backbonding may play a more important role.

We found that $|\Delta H_{\text{XB}}^0[\text{TS}]|$ also correlates with Δq on 3F. However, there are two separate correlations, one for electron-withdrawing substituents and another for electron-donating substituents (Figures S6a and S6b). The exact reason for two separate correlations is unclear, however we observe that the electron-donating sets have an average D···I distance that is 0.078 Å greater than that for the electron-withdrawing sets, so we speculate that it might be because $|\Delta H_{\text{XB}}^0[\text{TS}]|$ becomes less sensitive to changes in NPA charges on 3F (i.e. the slope decreases) when the donor and acceptor become close enough beyond a critical D···I distance. Nevertheless, these correlations can suggest that $|\Delta H_{\text{XB}}^0[\text{TS}]|$ primarily depends on a shift of charge from electron acceptor to donor, in other words via a backbonding pathway.

We next explain the decomposition of Figure S6a in more detail and our rationale for how the correlations in Δq suggest the flow of electron density from the diiodomethane TS to PF_3 . Starting from a correlation plot of Δq for Nu vs. C[E] and LG vs. C[E] (Figures S8a, S8b), we see that a decrease in electron density on Nu and LG ($\Delta q \approx +0.005$ to $+0.035$) correlates well with an increase in electron density on C[E] ($\Delta q \approx -0.007$ to -0.03). With Nu and LG both being a terminal group, this implies that electron density flows out of Nu and LG and at least part of that electron density ends up on C[E]. When we try to correlate Δq on C[E] with that on I[XB] (Figure S8c), we find that the gain in electron density on C[E] correlates with a gain in electron density on I[XB] ($\Delta q \approx -0.021$ to -0.048). The three correlation plots (Figures S8a – S8c) together suggest that there is electron density that flows from Nu and LG, via C[E], and onto I[XB]. We noted in the main text that $\Delta q < 0$ for 3F, and to determine where that gain in electron density might have come from, we tried to correlate Δq on 3F vs. Δq on I[XB], C[E], Nu, and LG (Figures S8d – S8g). What we found was a more complicated picture where we cannot confidently conclude that the gain in electron density on 3F comes from the gain in electron density on I[XB]. We were able to extract a correlation for the

sets with electron withdrawing groups (excluding (CN, CH₃) for plots with I[XB] and LG), but not for the sets with electron donating groups. We do question the rigor of such results and their utility is open for further investigation. However, we discuss what we were able to obtain and try to infer from them what they might suggest about electron movement in the XB adduct between the diiodomethane and PF₃. We see that, the loss in electron density on Nu and LG does correlate with the gain on 3F, and the gain in electron density on C[E] correlates with the gain on 3F. While we cannot conclude directly that the correlation observed implies causation, the close vicinity of these groups as well as the results of orbital analysis in the main text and Sections 3.4 and 4.5 of this document can suggest that there is contribution from Nu, LG, and C[E] for the gain in electron density on 3F. For I[XB] vs. 3F (Figure S8f), since 3F is a terminal group, the negative correlation can imply that I[XB] passes on more electron density to 3F than it receives from C[E], leading to a less negative Δq on I[XB] correlating with a more negative Δq on 3F. While $\Delta q > 0$ for the sum of all atoms on PF₃, which indicates that σ -donation is present, as $\Delta H_{XB}^0[TS]$ becomes more negative, the sum of Δq on all atoms of PF₃ decreases (becomes less positive; Figure S7a) and Δq becomes more negative on 3F (Figure S7b). This implies that even if there is a net transfer of electron density out of PF₃, it is the transfer of electron density *into* it, which makes the Δq less positive, that determines the magnitude of $\Delta H_{XB}^0[TS]$.

The flow of electrons from Nu and LG towards C[E] and I[XB] on the diiodomethane TS, as demonstrated by $\Delta q > 0$ on Nu and LG negatively correlating with $\Delta q < 0$ on C[E] and Δq on C[E] positively correlating with $\Delta q < 0$ on I[XB], suggest that electron density is moving towards PF₃. From chemical intuition, the driving force for that movement is likely a low-lying, π -symmetric σ_{P-F}^* on PF₃. The complex relationship of Δq on 3F vs. other atoms can suggest that the contribution towards π -backbonding is not well defined from a particular atom, but perhaps from regions of electron density, across a number of atoms on the diiodomethane TS, with compatible symmetry and energies that can interact with the σ_{P-F}^* that contribute to a overall stabilization of the XB adduct. Orbital analysis and density of states around the HOMO, then, allow us to further investigate the contribution of π -backbonding towards XB.

We also note here that using $E^{(2)}$ within the NBO framework for the π interaction between the diiodomethane TS and PF₃ turned out not to be the best way to examine the backbonding interaction. The observable backbonding interaction is small and comes from the interactions between the lone pair of the

halogen-bonding iodine and three separate P-F antibonding orbitals. The localized nature of NBO partitions the π^* of PF₃ into three separate P-F antibonding orbitals and other localized orbitals that together form the π^* MO. In principle, the sum of $E^{(2)}$ from the donor p orbitals on the diiodomethane and all the partitioned acceptor orbitals have to add up to a reasonably large value should backbonding be significant. However, the small backbonding interaction observed is likely because of poor orbital overlap in many of these interactions that result in E^2 values that are below the printing threshold ($E^{(2)} = -\frac{q_i|F_{ij}|^2}{\varepsilon_j - \varepsilon_i}$ where F_{ij} is small).

2.1.2 NH₃

In contrast to what we observed for PF₃, when NH₃ is the electron donor, we observe results that support the traditional, σ -type XB interaction, directional from NH₃ to the diiodomethane TS, as the primary mode for XB stabilization. The expansion of TS observed for NH₃ involves the Nu \cdots C[E] and LG \cdots C[E] bond lengths increasing by around 0.01 to 0.1 Å (Figure S3b), which is supported by $\Delta q < 0$ on Nu, LG, and C[E]. More negative values of Δq seems to correlate with the increase in the bond lengths (Figure S9), but we explain on the next page that there may be a more complicated situation involved. We also find (Figure S10b) that $|\Delta H_{\text{XB}}^0[\text{TS}]|$ correlates with $\Delta q > 0$ on the 3 hydrogen atoms of NH₃ (3H). This suggests that when NH₃ is the electron donor the primary contribution for $\Delta H_{\text{XB}}^0[\text{TS}]$ is a shift of charge from electron donor towards acceptor, which is consistent with the correlation between $\Delta H_{\text{XB}}^0[\text{TS}]$ and $E^{(2)}[\sigma^*]$.

According to Figure S4b, $\Delta q > 0$ occurs on I[XB] and 3H, while $\Delta q < 0$ occurs on Nu, LG, C[E], and the nitrogen atom of NH₃ (N). The sum of groups with positive Δq negatively correlates with the sum of groups with negative Δq (Figure S10a). While there is a net increase of electron density on N ($\Delta q \approx -0.001$ to -0.009), there is an overall decrease of electron density on the entire NH₃ molecule ($\Delta q \approx +0.019$ to $+0.048$). The decrease comes entirely from 3H ($\Delta q \approx +0.022$ to $+0.050$). The decrease of electron density on NH₃ along with the increase on C[E], Nu, and LG support that there is significant forward σ -donation from NH₃ to the diiodomethane. Since there is a significant decrease in electron density on the entire molecule of NH₃, this indicates that charge is being transferred out of the molecule. The only feasible pathway for this is via σ -donation from the nitrogen atom to the $\sigma_{\text{C}-\text{I}[\text{XB}]}^*$ of the diiodomethane. This is supported by the increase in the C-I[XB] bond length by around 0.005 to 0.02 Å. The initial movement of electrons away from the nitrogen atom towards the diiodomethane leads to polarization of the NH₃ molecule, with electron density from 3H moving towards N to compensate for the electron density moved out of it. The net increase of electron density on N means that NH₃ is polarized to an extent such that more electron density flows from 3H to N than from N to the $\sigma_{\text{C}-\text{I}[\text{XB}]}^*$ of the diiodomethane. This implies that some of that electron density on N is localized on it, and can interact with the σ -hole in an electrostatic fashion. The decrease on I[XB], we believe involves it not being able to hold the influx of electron density well, with more electron density being passed on to C[E], Nu, and I (mostly the latter two) than donated in from NH₃.

When trying to decompose Figure S10a, we find a more complicated picture (Figure S12). First, we observe a negative correlation between N and I[XB] (Figure S12d). At first, we were confused by $\Delta q < 0$ on N and $\Delta q > 0$ on I[XB], as this could be interpreted as a flow of electron density from I[XB] to N, yet it's unlikely due to the high-energy σ^* of NH₃. After seeing that the sets with electron-withdrawing groups have smaller magnitudes of Δq , we believe that the negative correlation comes from increased forward σ -donation that has a bit but not quite overcome the negative Δq brought about by the electron density localized on N, which came from polarization within NH₃ and is involved in an electrostatic interaction with the $\sigma_{C-I[XB]}^*$. For I[XB] vs. C[E] (Figure S12c), we observe a positive correlation but the sign of Δq on C[E] depends on the electron-withdrawing or donating nature of the substituents involved. We see that the set (CH₃, CH₃) is far out in the $\Delta q > 0$ region. If we assume that the correlation holds, both I[XB] and C[E] having $\Delta q > 0$ means that the two groups are involved in passing on electron density due to a deficiency of electrons. However, if we disregard the sets that contain a CH₃ group (i.e. (CN, CH₃) and (CH₃, CH₃), we find that the remaining sets have $\Delta q < 0$ for C[E]. For these sets, we then have I[XB] acting like a terminal electron source with C[E] acting like a terminal electron drain. For C[E] vs. Nu (Figure S12a), and C[E] vs. LG (Figure S12b), in addition to the sign of Δq for C[E], the type of correlation we observe also depends on the nature of the substituents. If we consider all the sets, we see a negative correlation, but if we again disregard the sets that contain a CH₃ group, we get a positive correlation. The latter, however, is a much stronger correlation. Either way, even though we are unclear about the exact mechanism of how the electrons move from NH₃ through the TS and eventually to Nu and LG, $\Delta q < 0$ on both Nu and LG is consistent with the idea that both groups are being pushed further away from C[E] due to extra electron density from NH₃ (i.e. the expansion of TS). The exact reason why the magnitude of Δq for (CH₃, CH₃) is so much larger than the other sets, which is basically what led to the negative correlation described earlier, is unclear. However, we postulate that, since it's the most electron-donating of all the sets, perhaps it has surpassed a critical "amount of electron richness" in the diiodomethane where large changes are induced by the XB interaction.

2.1.3 CO

For CO as the electron donor, we find that the changes in the Nu \cdots C[E] and LG \cdots C[E] bond lengths are about a magnitude smaller, increasing only by around 0.001 to 0.015 Å (Figure S3c). Disregarding the data with more than one imaginary frequency in the TS, the decrease in Δq exhibits a moderate correlation with an increase in the bond lengths (Figure S13). Following a similar line of reasoning established earlier, this may indicate that σ donation might have a greater effect in the TS here. The changes in NPA charges follow a similar direction as those for NH₃, however their magnitudes are similar to those observed for PF₃ (Figure S4c). From the results for CO, we observe results that support both σ -type forward donation as well as π -backbonding. However, given that $\Delta H_{XB}[\text{TS}]$ correlates well with $E^{(2)}[\sigma^*]$ for forward σ -donation and NPA analysis doesn't reveal any significant correlations for π -backbonding, we believe that forward σ -donation is the primary contributor towards the XB stabilization while the effect of π -backbonding on $\Delta H_{XB}[\text{TS}]$ is less well-defined compared to that on PF₃.

According to Figure S4c, $\Delta q > 0$ for I[XB] and the carbon atom of CO C[=O], while $\Delta q < 0$ for Nu, LG, C[E], and the oxygen atom of CO (O). The sum of groups with positive Δq negatively correlate with the sum of groups with negative Δq (Figure S14a), which indicates that in general charge is being transferred from the former to the latter. In addition, $\Delta q > 0$ for the sum of both atoms on the CO molecule, indicating that there is a net amount of electron density being transferred out of the molecule. The direction of this charge transfer is from CO to the diiodomethane, supporting the presence of forward σ -donation. However, its magnitude is much smaller ($\Delta q \approx +0.007$ to $+0.013$) compared to that for NH₃ and PF₃. In addition, unlike the correlation we observed for Δq on Y (N for NH₃, C[=O] for CO) vs. I[XB] when NH₃ is the electron donor, we did not observe a significant correlation between C[=O] and I[XB]. The small Δq and the lack of a correlation suggest that charge transfer is not the major contributor towards the σ -type XB but instead we believe that it involves more contribution from electrostatic interactions between C[=O] and I[XB]. This makes sense if we consider that electrons on C[=O] are much more localized on it (due to the electronic structure of CO) compared to electrons on N of NH₃.

$\Delta q < 0$ for I[XB] and O also suggest that there is electron flow from the diiodomethane to CO. With CO as a strong π -acceptor, it is feasible that there is backbonding from the diiodomethane to the π^* of CO via a π -type pathway. A plot of $\Delta H_{\text{XB}}[\text{TS}]$ vs. Δq on O reveals a moderate negative correlation between the two quantities (Figure S15b). Unlike that observed for PF_3 , larger increases in electron density on O correlate with smaller $\Delta H_{\text{XB}}[\text{TS}]$ values, suggesting that the increase in electron density on O is somehow related to *destabilization* of the transition state. However, Δq on O does not correlate with Δq on any of the other atoms considered in our NPA analysis (Figure S16d – S16g), which means that we cannot conclude whether the increase in electron density on O is due to π -backbonding or polarization within the CO molecule. Since $\Delta H_{\text{XB}}[\text{TS}]$ correlates well with $E^{(2)}[\sigma^*]$ for forward σ -donation, we believe that π -backbonding is likely not the primary contributor towards XB here and its effect is less well-defined than that observed for PF_3 . Why would CO, despite being a strong π -acceptor, not have a significant π -backbonding interaction here? We believe the large energy and size differences between the iodine 5p orbitals and the localized π^* of CO leads to little electron transfer from diiodomethane to CO at the donor-acceptor distances for the XB interactions investigated in this study (i.e. 3 – 3.5 Å here vs. 2 – 2.5 Å for transition metal complexes). It is likely then, that electrostatic interactions between C[=O] and the σ -hole of the diiodomethane serve as the primary contributor towards the XB stabilization.

2.2 More discussion on charge decomposition analysis

We employed charge decomposition analysis (CDA) developed by Dapprich and Frenking (ref. 38 in main text) and later expanded by Xiao and Lu (ref. 39 in main text) to investigate the amount of electron density transferred from diiodomethane to PF₃ via each π -type bonding orbital shown in Figure 3a of the main text and Section 3.4.1 in this document, as well as the contribution of π -type orbitals from each fragment to the π -type MOs observed in the complex.

The CDA method is useful for identifying the contributions from individual MOs of the complex orbitals towards the total amount of electron density transferred from one fragment to another. Dapprich and Frenking derived that for an arbitrary basis Φ (in our case MOs on the fragments),

$$d_i = \sum_{m \in M}^{\text{occ},M} \sum_{n \in N}^{\text{vac},N} \eta_i c_{m,i} c_{n,i} \langle \Phi_m | \Phi_n \rangle \quad (\text{Eq. S1})$$

$$b_i = \sum_{m \in M}^{\text{vac},M} \sum_{n \in N}^{\text{occ},N} \eta_i c_{m,i} c_{n,i} \langle \Phi_m | \Phi_n \rangle \quad (\text{Eq. S2})$$

where d refers to the amount of charge donated from fragment M to N, b the amount of charge back-donated from fragment N to M, i the index for MOs of the complex, m and n the index for MOs of the fragments, η the occupation number, and c the coefficient of fragment MO m or n in complex MO i . The terms “occ” and “vac” refer to occupied and vacant orbitals, respectively. With M taken as the Lewis base and N the Lewis acid (diiodomethane), one can identify the amount of charge transfer from M to N contributed by each complex MO. For each complex MO, one can also compute the contributions of the fragment MOs that contribute to the d and b of that complex MO. This allows one to reveal whether a complex MO is primarily formed from mixing a certain pair of fragment MOs, with one MO from each fragment, or from more than one MO on each fragment.

Tables S18 is the expanded version of Table 1 in the main text, and Table S19 the detailed analysis of the π contribution using CDA. We adopt the following nomenclature for the terms used in the heading of the tables:

$$\rho_{<>}^{[]}$$

when $[] = D$, the term refers to d_i from Equation S1, and when $[] = A$, the term refers to b_i from Equation S2; $<> = \sigma$ refers to the σ interaction (we take the σ orbital having the largest contribution towards charge transfer from PF_3 to diiodomethane), and $<> = \pi$ refers to the π interaction. A notation “[frag]” is added after the term to indicate that we are referring to the contribution of specific π -type fragment MOs (see Table S19 for orbital indices) towards the values obtained for the π -type complex MOs. The Σ refers to the sum over the four complex MOs noted for each (R_1, R_2) shown in Table S19.

The large $\frac{\sum \rho_{\pi}^4[\text{frag}]}{\sum \rho_{\pi}^4}$ term (shown in both Table S18 and S19) confirms that a significant portion of backdonation from PF_3 to diiodomethane (i.e. contribution to the π -type complex MO) is indeed due to interactions between specific π -type MOs from each fragment, thereby supporting the necessity for π -type orbitals interactions for the backbonding interactions involved in this study.

3. Figures

Note on Figures 1, 2, and S1, S2, S13 – S16: For the TS with CO as the electron donor, while we were unable to arrive at structures without two additional imaginary modes for the sets of substituents (H, H), (H, CH₃), and (CN, CH₃), the imaginary modes are all < -15 cm⁻¹ and the results for these sets of substituents exhibit a consistent trend from the rest of the data. According to Figure 1 in the main text, these TS structures with the extra imaginary modes have a consistent, vertical offset for $\Delta H_{XB}[\text{TS}]$, and Figure 3 also shows a consistent offset in the data for these sets of substituents. For GS with NH₃ as the electron donor with (H, H) as the substituents, we were unable to arrive at a structure without an imaginary mode that is < 10 cm⁻¹. However, the energetic data of that set of substituents exhibited no significant deviation from the overall trend across the different substituents. For all of the cases mentioned above, we tried tightening the convergence criteria as well as changing the initial geometry, but were unable to converge, formally, to a first-order saddle point for the TS and an electronic minimum for the GS. Despite this, from the data we believe that the small imaginary modes and its consistent (for CO) and insignificant (for NH₃) effect on the energetic data of the corresponding structures still allow us to make meaningful comparisons between the different electron donors on the effect of XB and thus do not affect the overall picture and conclusions of our study.

3.1 $\Delta G_{\text{XB}}^{\ddagger}$ vs. $\Delta G_{\text{ref}}^{\ddagger}$ and ΔH_{XB}^0 vs. $E^{(2)}[\sigma^*]$

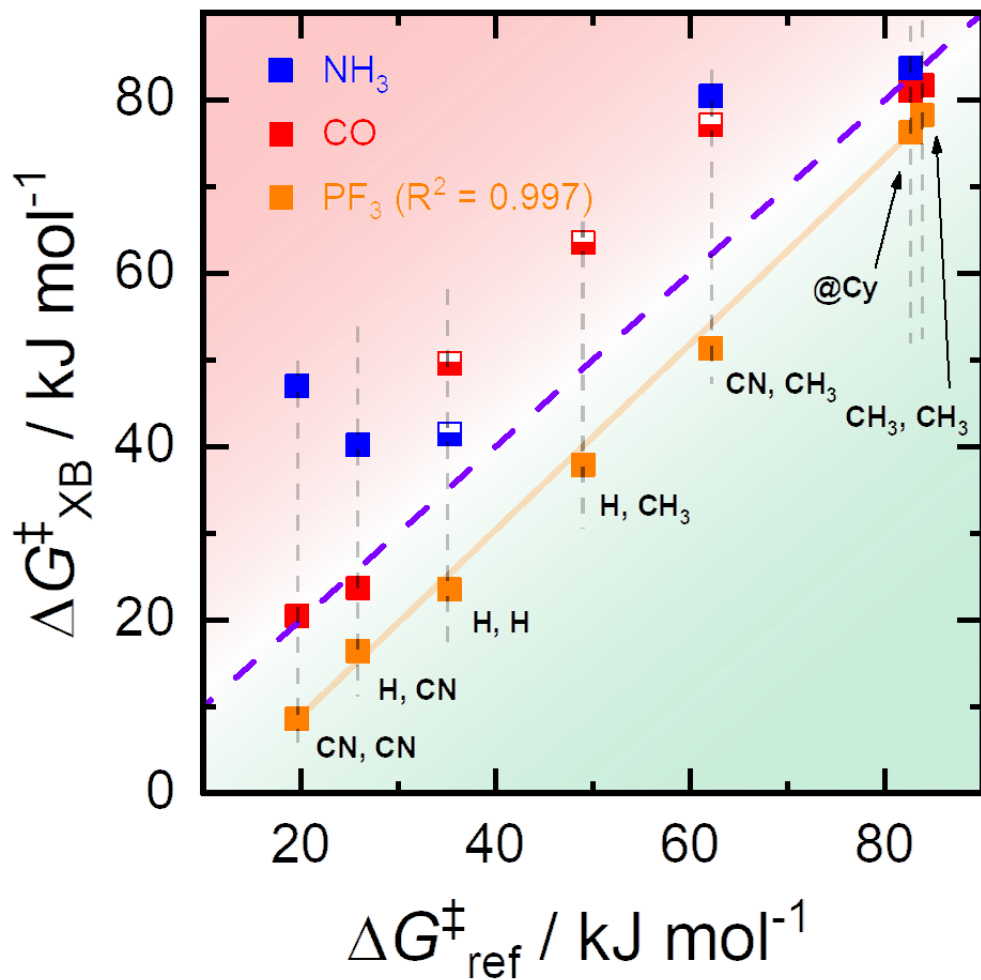


Figure S1. Plot of $\Delta G_{\text{XB}}^{\ddagger}$ vs. $\Delta G_{\text{ref}}^{\ddagger}$. The meaning of half-filled squares is the same as those in Figure 2 of the main text.

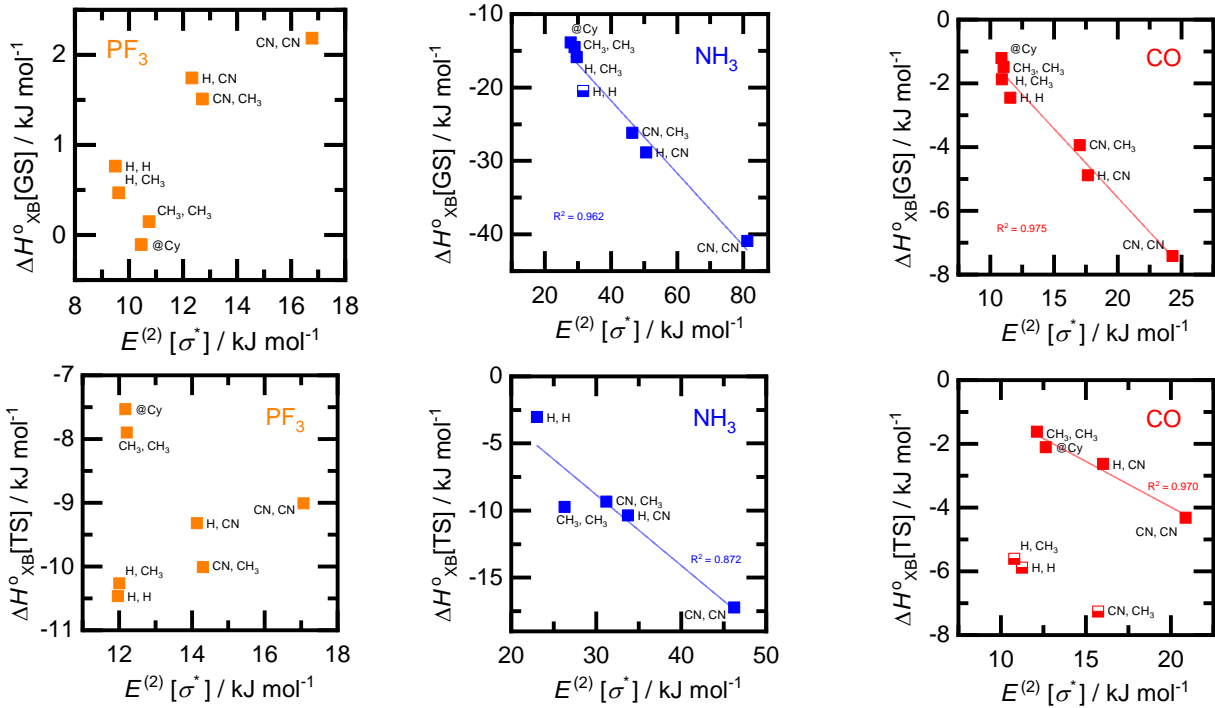


Figure S2. Correlation plots of $\Delta H_{XB}^0[\text{GS}]$ (top) and $\Delta H_{XB}^0[\text{TS}]$ (bottom) vs. $E^{(2)}[\sigma^*]$ for the three electron donors. Half-filled squares have the same meaning as those indicated in Figure 2 (main text). For TS with NH₃ as the electron donor, no data was plotted for (H, CH₃) and (@Cy) since no XB was present for those cases.

3.2 Changes in bond lengths and NPA charges for CO and NH₃ as electron donors

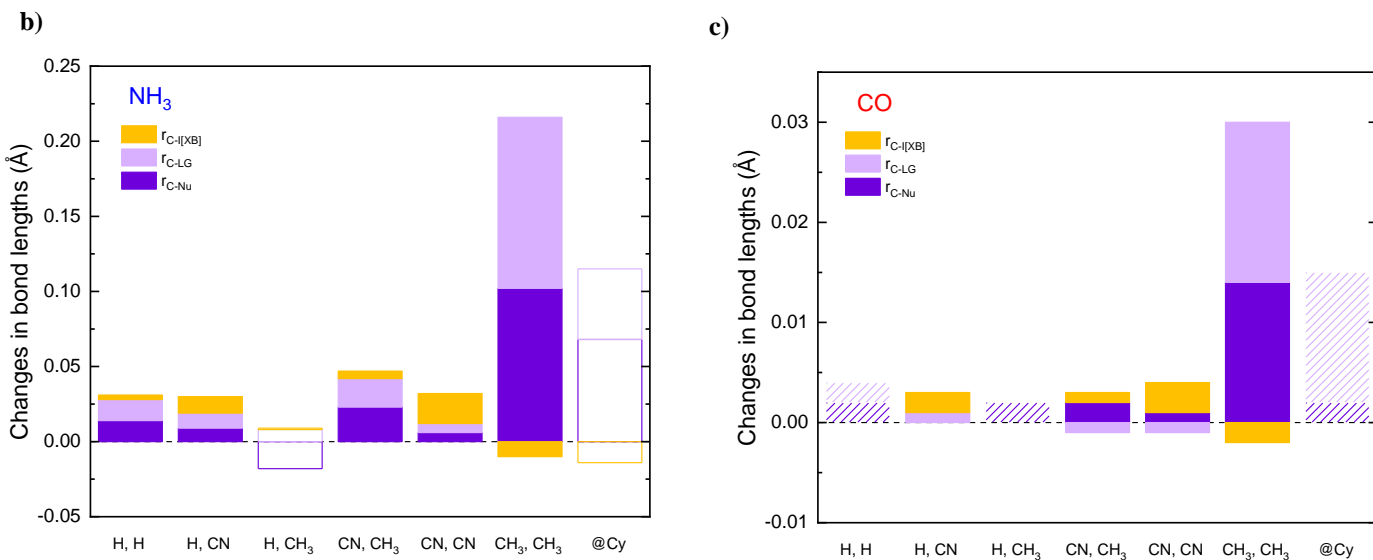
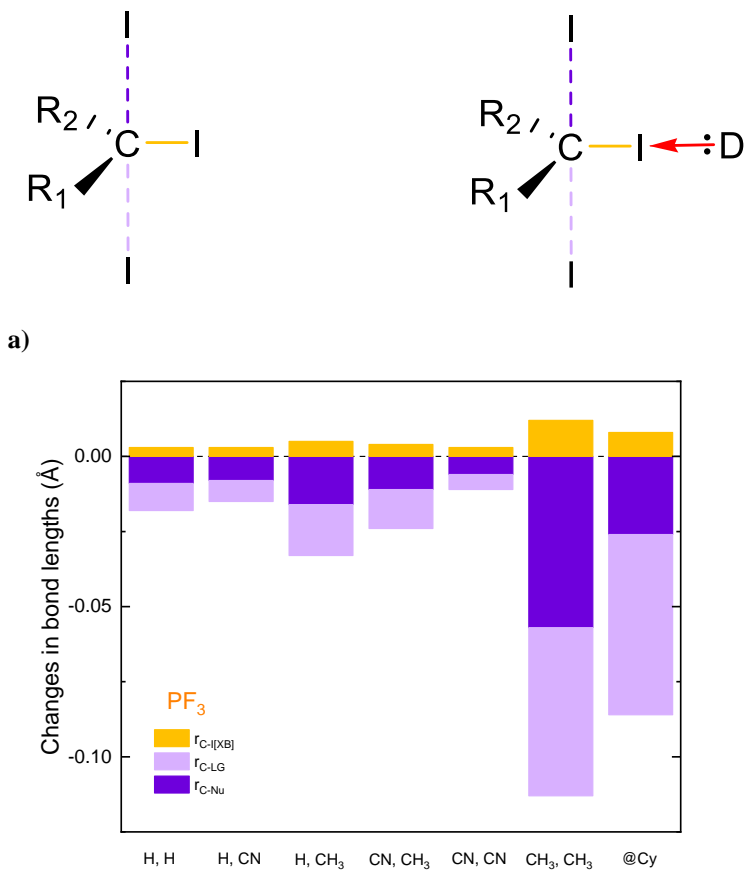


Figure S3. Changes in bond lengths between the electrophilic carbon and I[XB] (yellow), Nu (dark purple), and LG (light purple) going from no XB to XB for the following electron donors: **a)** PF₃, **b)** NH₃, and **c)** CO. For CO, the dashed lines indicate cases where more than 1 imaginary frequency is present in the transition state (see Table S6 for details). For NH₃, the unfilled boxes indicate cases with no XB in the transition state.

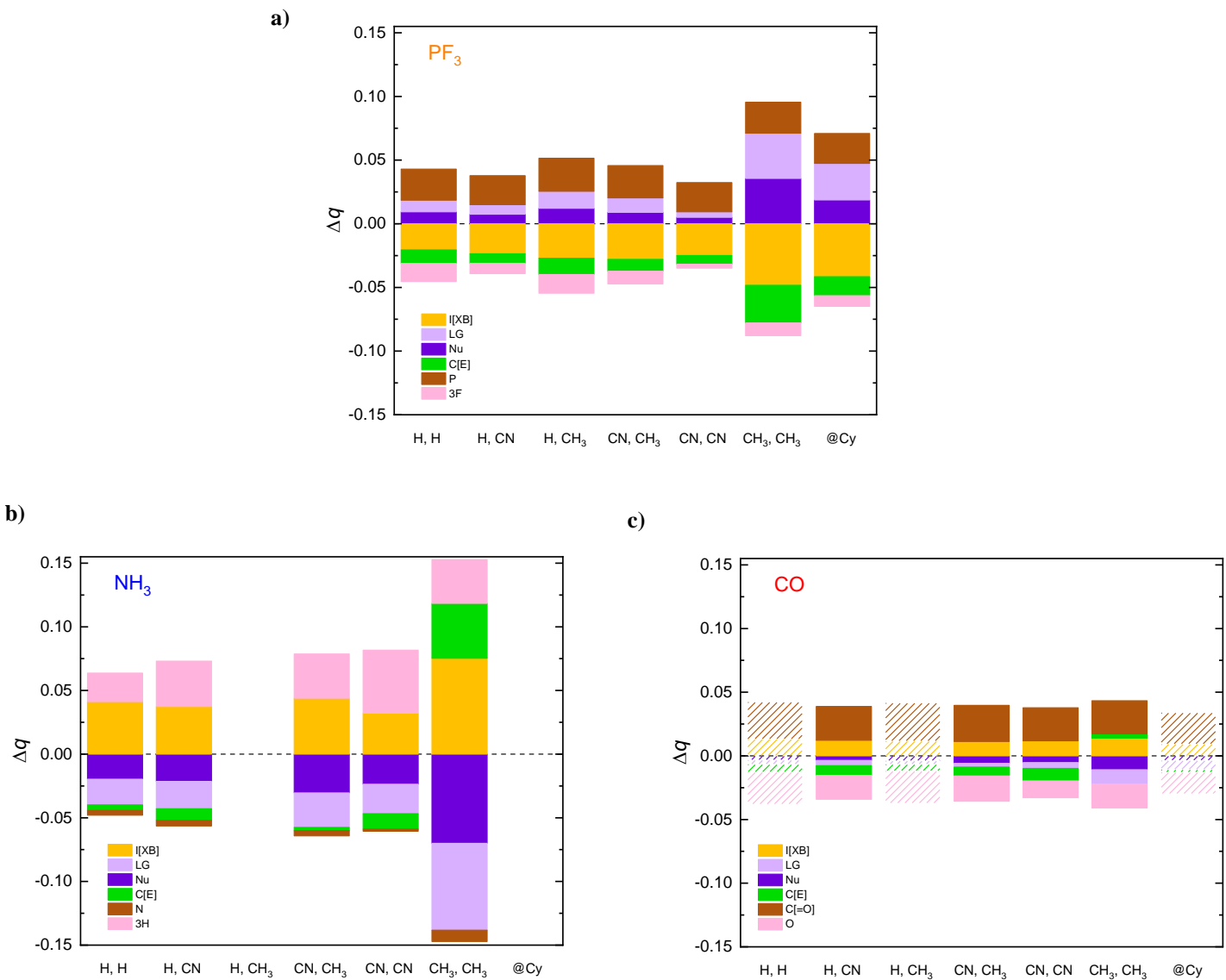
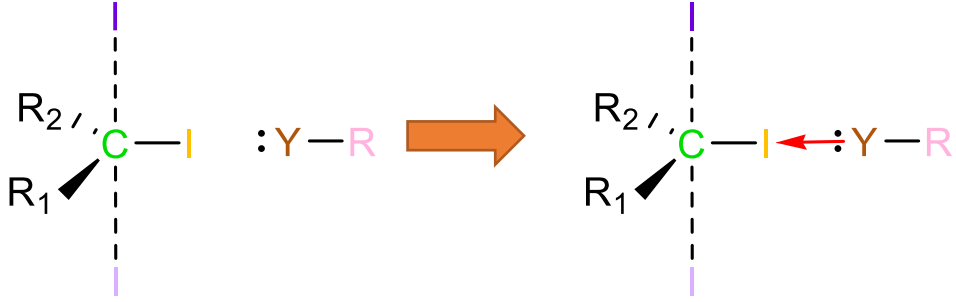


Figure S4. Changes in NPA charges on key atoms going from no XB to XB for the following electron donors: **a)** PF₃, **b)** NH₃, and **c)** CO. Dashed lines in the top panel indicate cases with more than 1 imaginary frequency in the transition state (see Table S6 for details), and the absence of plotted data for (H, CH₃) and (@Cy) in the bottom panel are due to no XB being present, making it meaningless to plot data for those cases.

3.3 NPA correlation plots

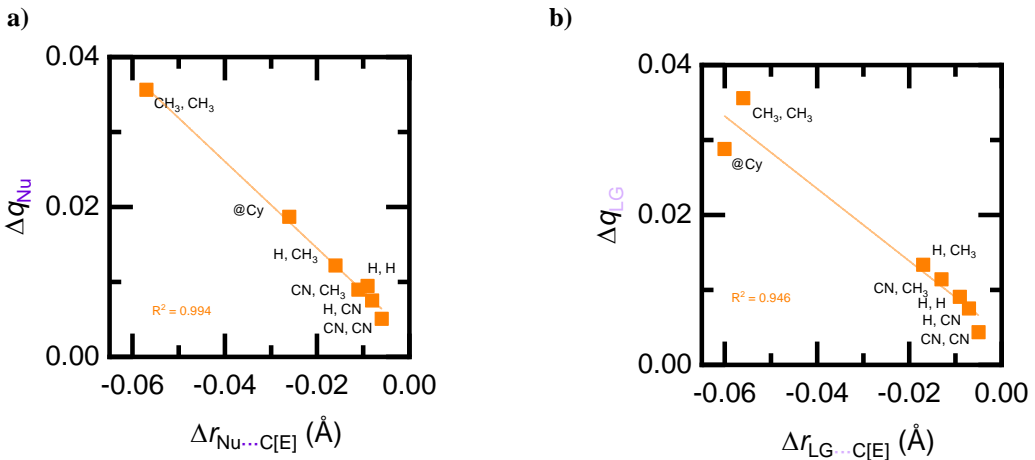


Figure S5. Correlation plots, with PF_3 as the electron donor, for **a)** Δq on Nu vs. the changes in bond distance between Nu and C[E], and **b)** Δq on LG vs. the changes in bond distance between LG and C[E].

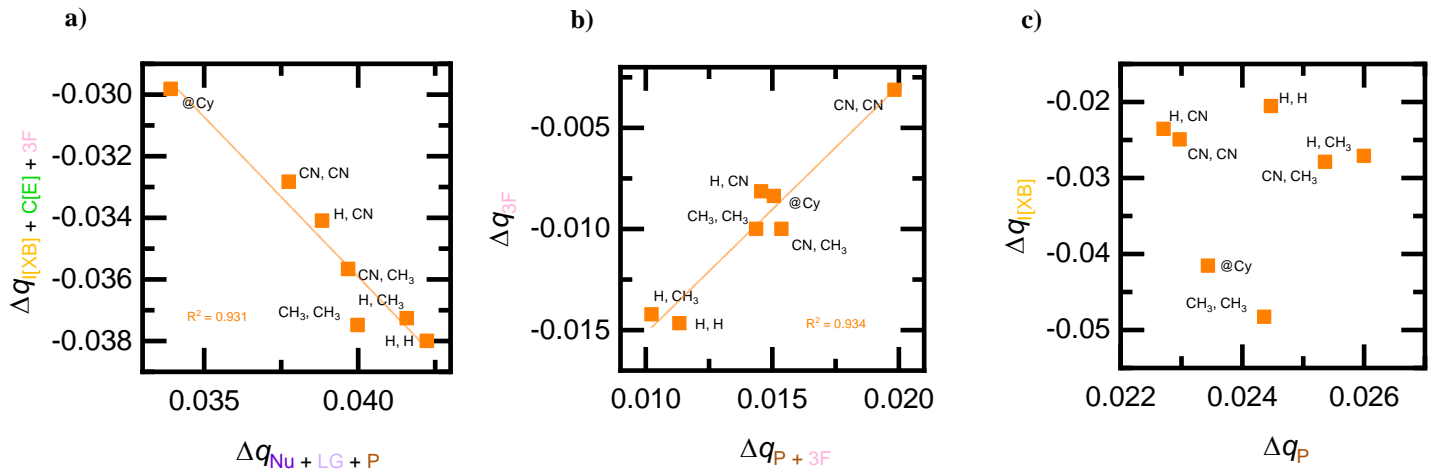


Figure S6. Correlation plots, with PF_3 as the electron donor, for **a)** the sum of Δq on groups with $\Delta q < 0$ vs. that on groups with $\Delta q > 0$, and **b)** Δq on 3F vs. sum of Δq on all atoms of PF_3 , **c)** Δq on $I[\text{XB}]$ vs. that on P. For **b)**, we note here that the description for the meaning of positive or negative correlations of Δq of two groups do not apply here as the same group (3F) appears in both the x and y axes.

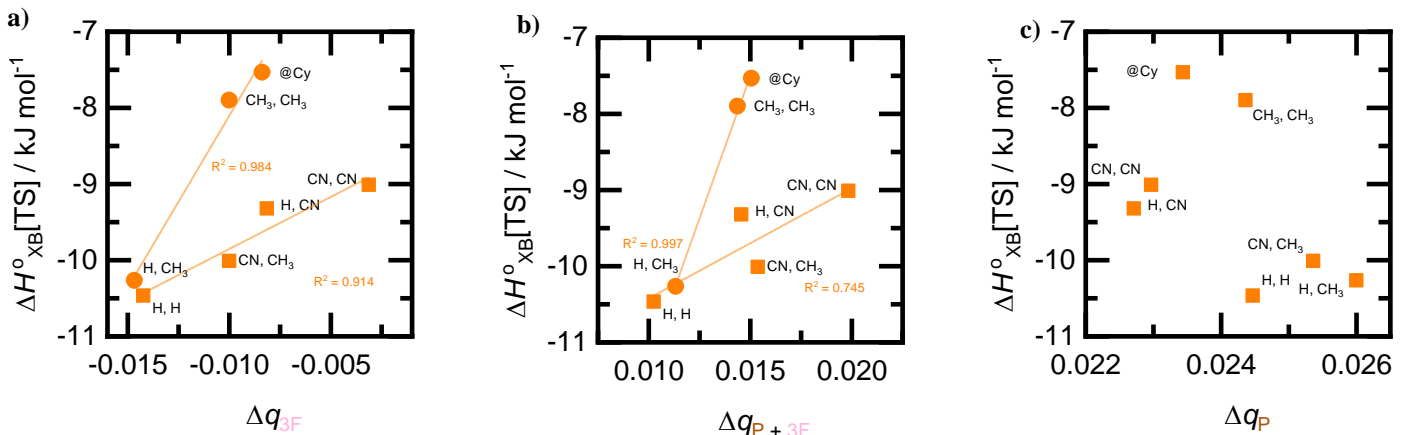


Figure S7. Correlation plots, with PF_3 as the electron donor, for $\Delta H_{\text{XB}}^0[\text{TS}]$ vs. Δq on **a)** the sum of all atoms on PF_3 , **b)** 3F, and **c)** P. For **a)** and **b)**, circles represent electron-donating groups and squares represent electron-withdrawing groups.

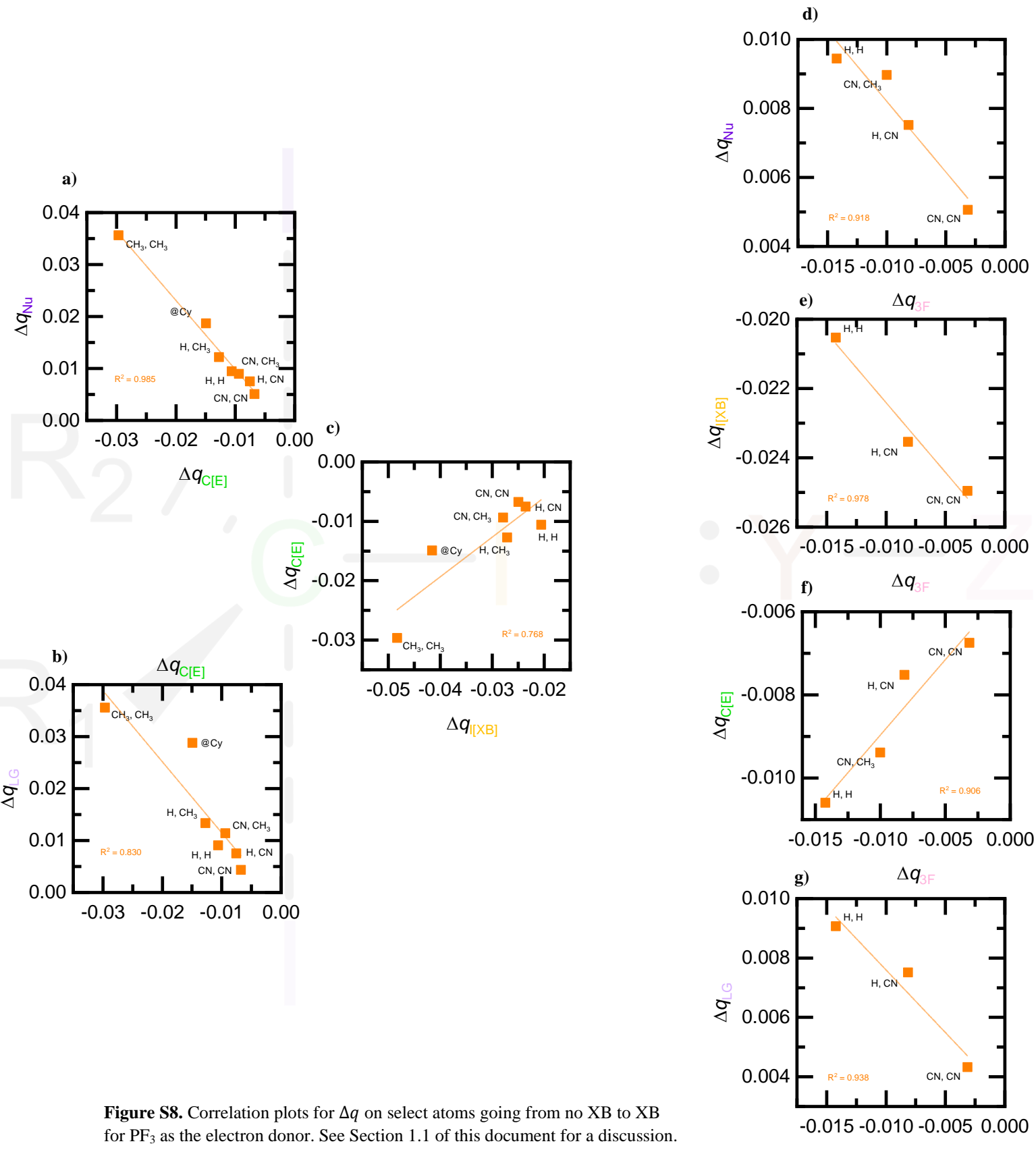


Figure S8. Correlation plots for Δq on select atoms going from no XB to XB for PF_3 as the electron donor. See Section 1.1 of this document for a discussion.

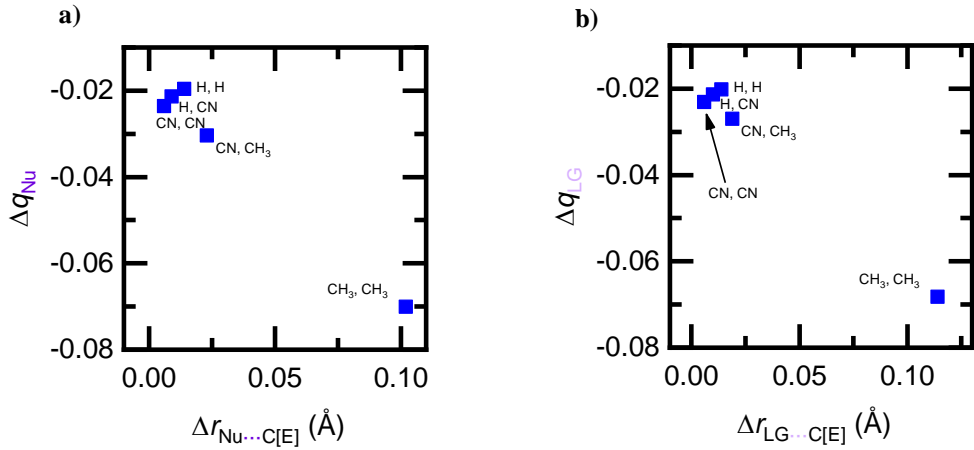


Figure S9. Correlation plots, with NH₃ as the electron donor, for **a)** Δq on Nu vs. the changes in bond distance between Nu and C[E], and **b)** Δq on LG vs. the changes in bond distance between LG and C[E].

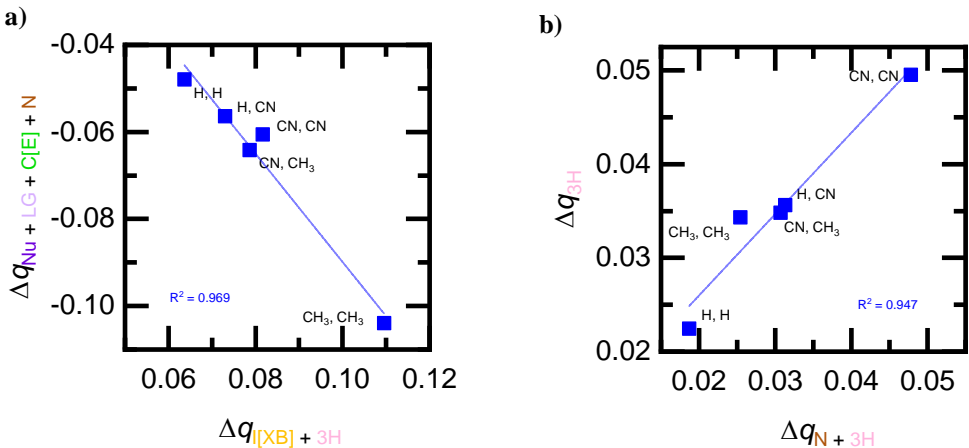


Figure S10. Correlation plots, with NH₃ as the electron donor, for **a)** the sum of Δq on groups with $\Delta q < 0$ vs. that on groups with $\Delta q > 0$, and **b)** Δq on 3H vs. sum of Δq on all atoms of NH₃. For **b)**, we note here that the description for the meaning of positive or negative correlations of Δq of two groups do not apply here as the same group (3H) appears in both the x and y axes.

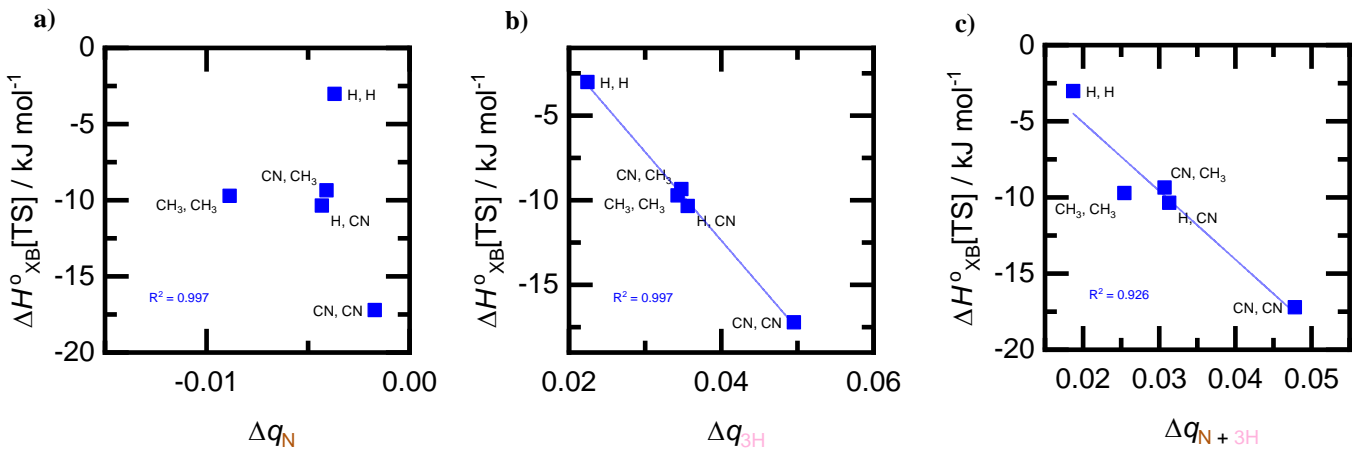


Figure S11. Correlation plots, with NH₃ as the electron donor, for $\Delta H_{\text{XB}}^0[\text{TS}]$ vs. Δq on **a)** sum of all atoms on NH₃, **b)** 3H, and **c)** N.

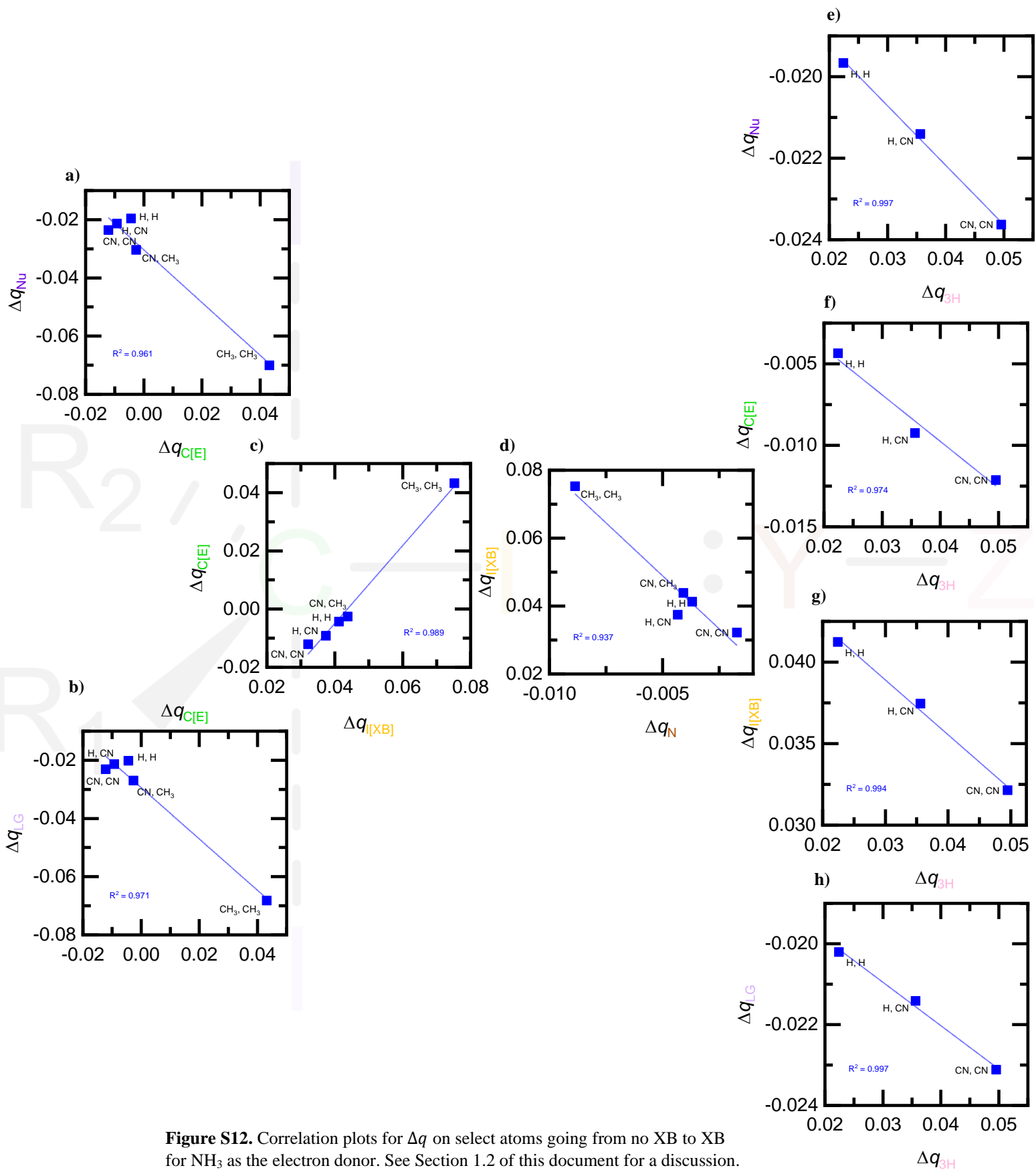


Figure S12. Correlation plots for Δq on select atoms going from no XB to XB for NH₃ as the electron donor. See Section 1.2 of this document for a discussion.

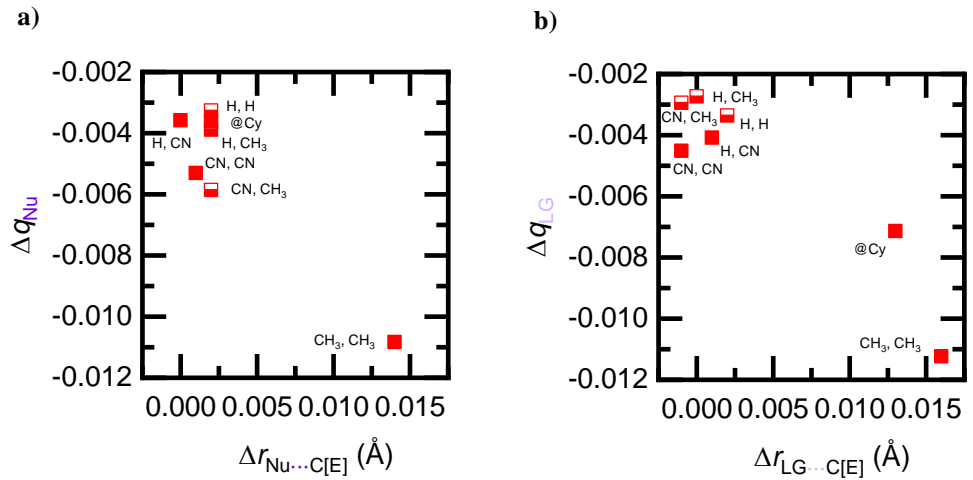


Figure S13. Correlation plots, with CO as the electron donor, for **a)** Δq on Nu vs. the changes in bond distance between Nu and C[E], and **b)** Δq on LG vs. the changes in bond distance between LG and C[E].

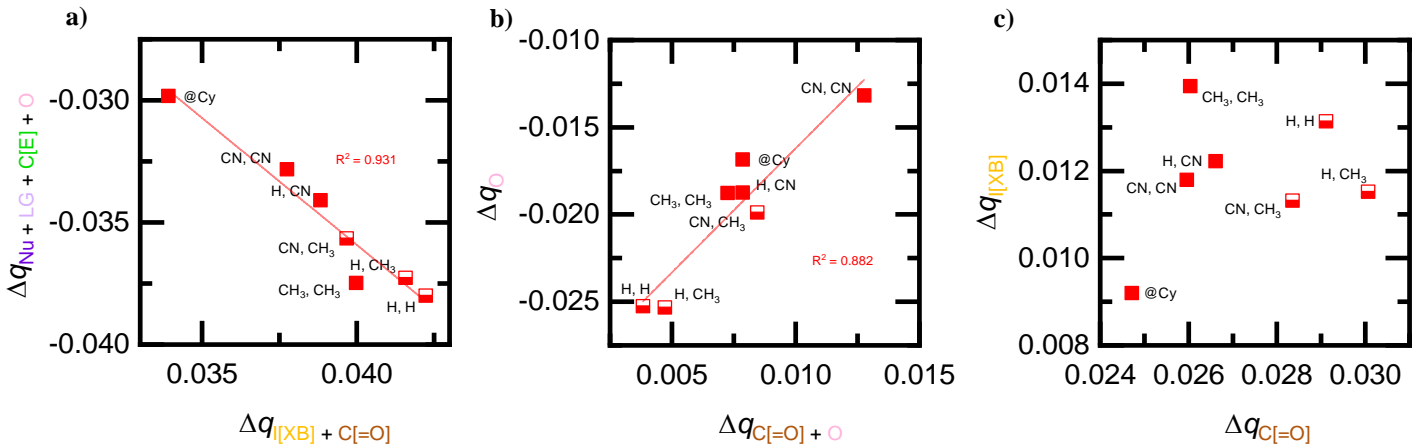


Figure S14. Correlation plot, with CO as the electron donor, for **a)** the sum of Δq on groups with $\Delta q < 0$ vs. that on groups with $\Delta q > 0$, **b)** Δq on O vs. sum of Δq on both atoms of CO, and **c)** Δq on I[XB] vs. that on C[=O].

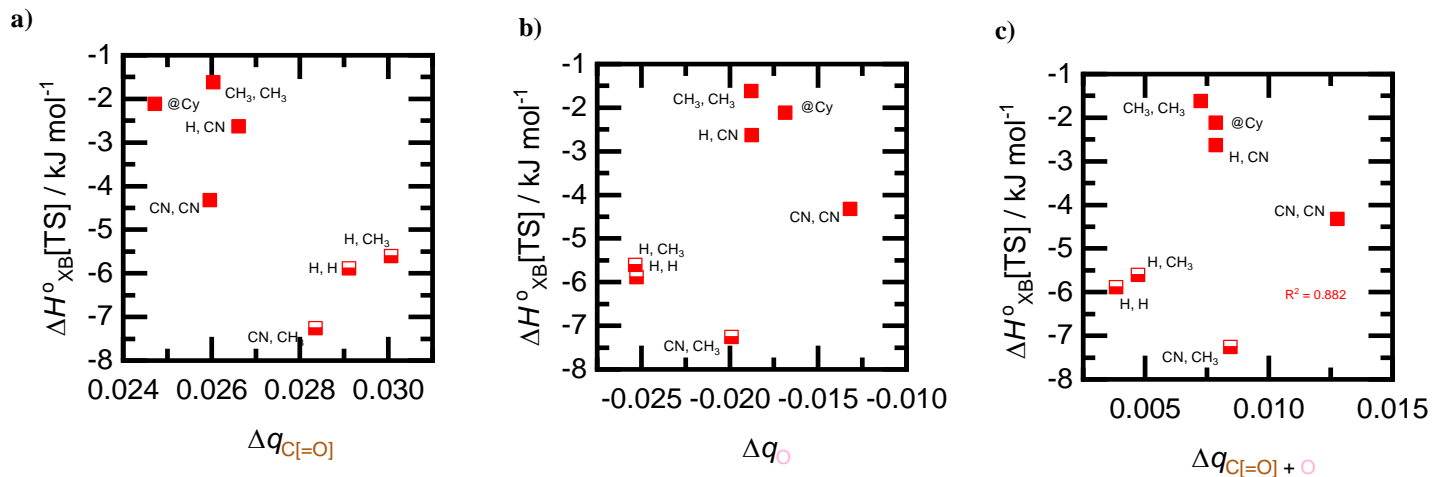


Figure S15. Correlation plots, with CO as the electron donor, for $\Delta H_{\text{XB}}^{\circ}[\text{TS}]$ vs. Δq on **a)** sum of all atoms on CO, **b)** O, and **c)** C[=O].

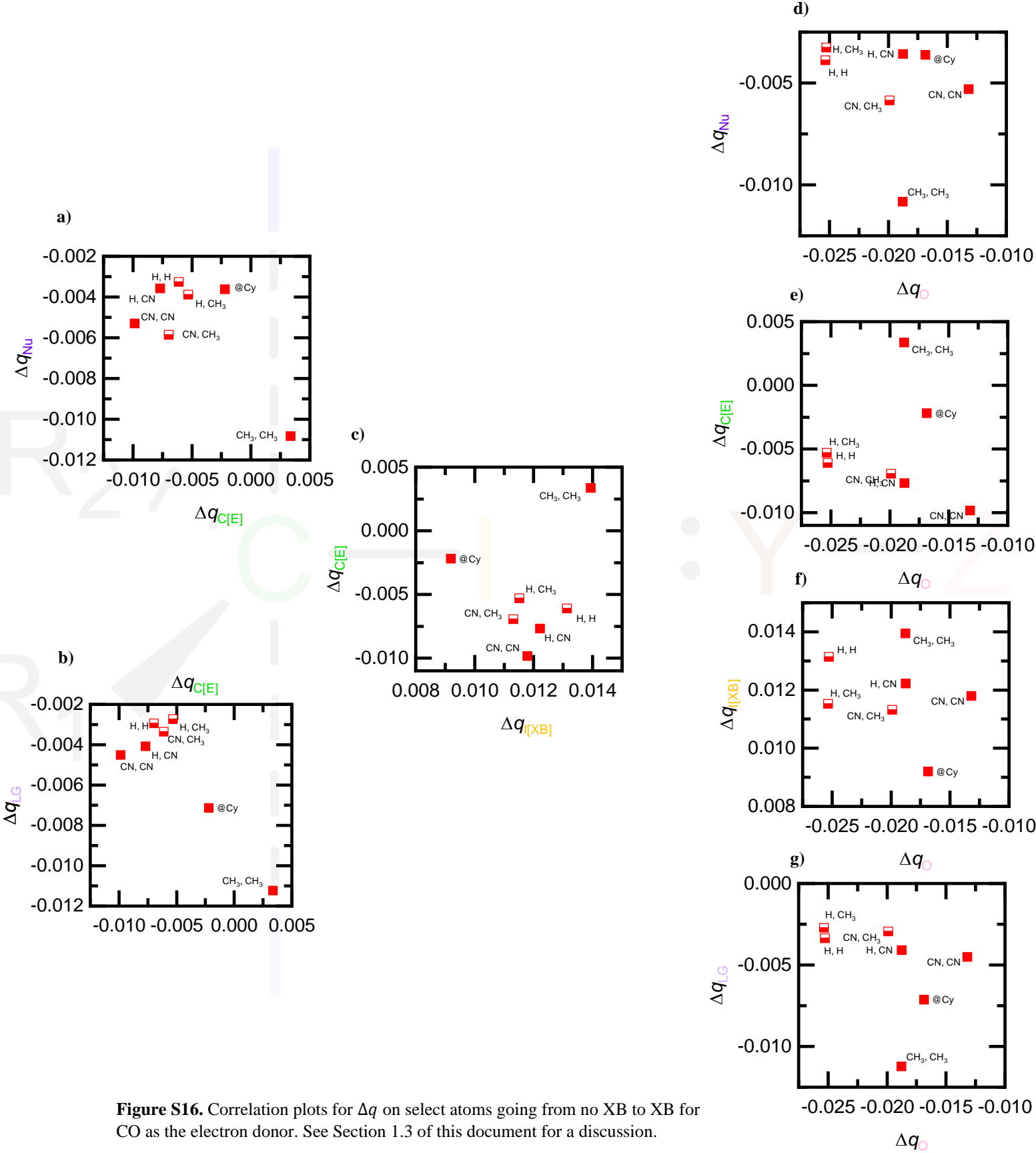


Figure S16. Correlation plots for Δq on select atoms going from no XB to XB for CO as the electron donor. See Section 1.3 of this document for a discussion.

3.4 π -type MO figures for all sets of substituents (calculated at M06-2X/def2-TZVP)
 3.4.1 PF₃ and NH₃

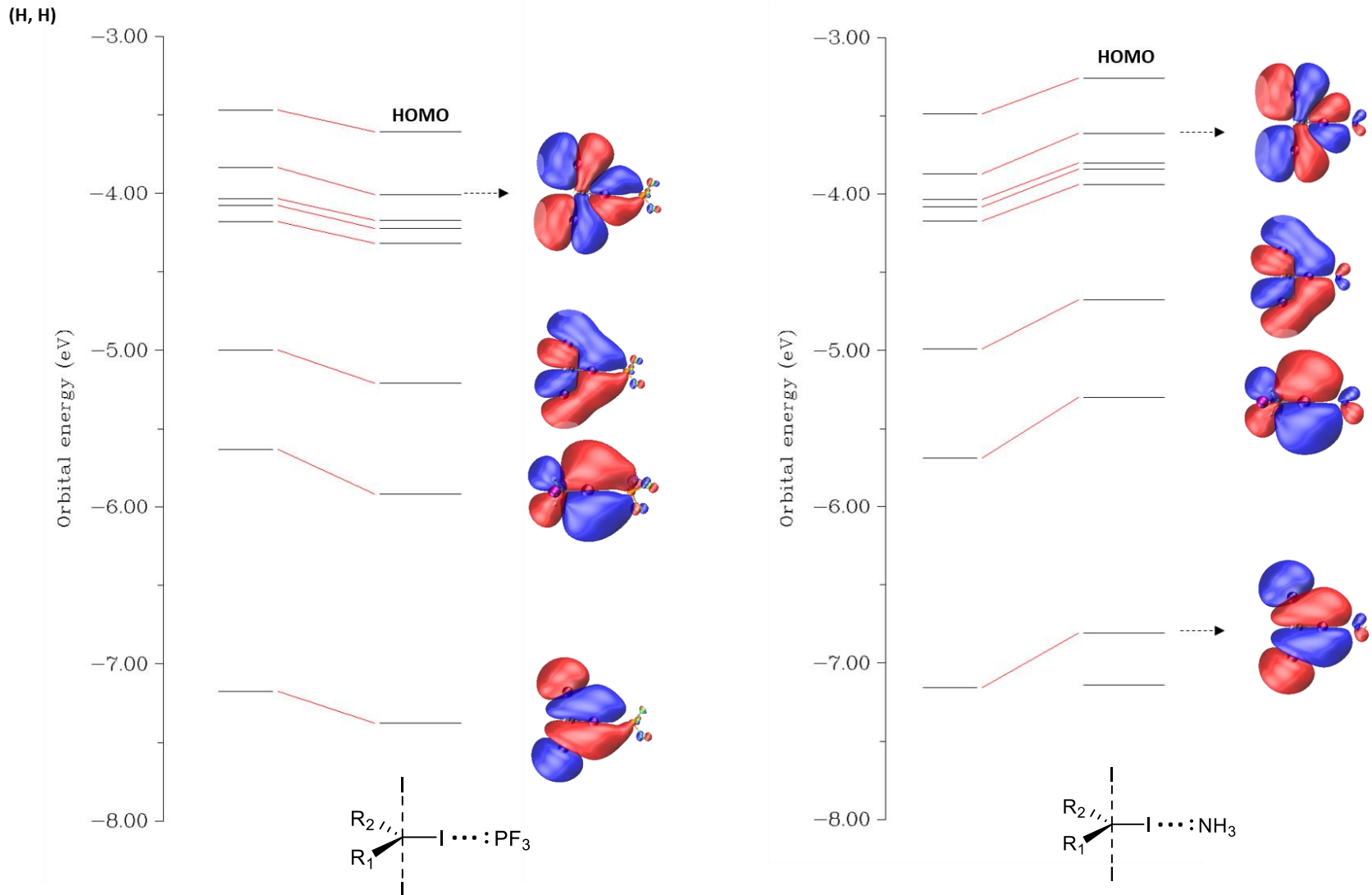


Figure S17. π -type molecular orbitals (MOs) involving backbonding from the diiodomethane to PF₃. The positions of each MO are indicated in the legend after the MO figures (HOMO = highest occupied molecular orbital). The MOs are visualized at an isosurface value of 0.002.

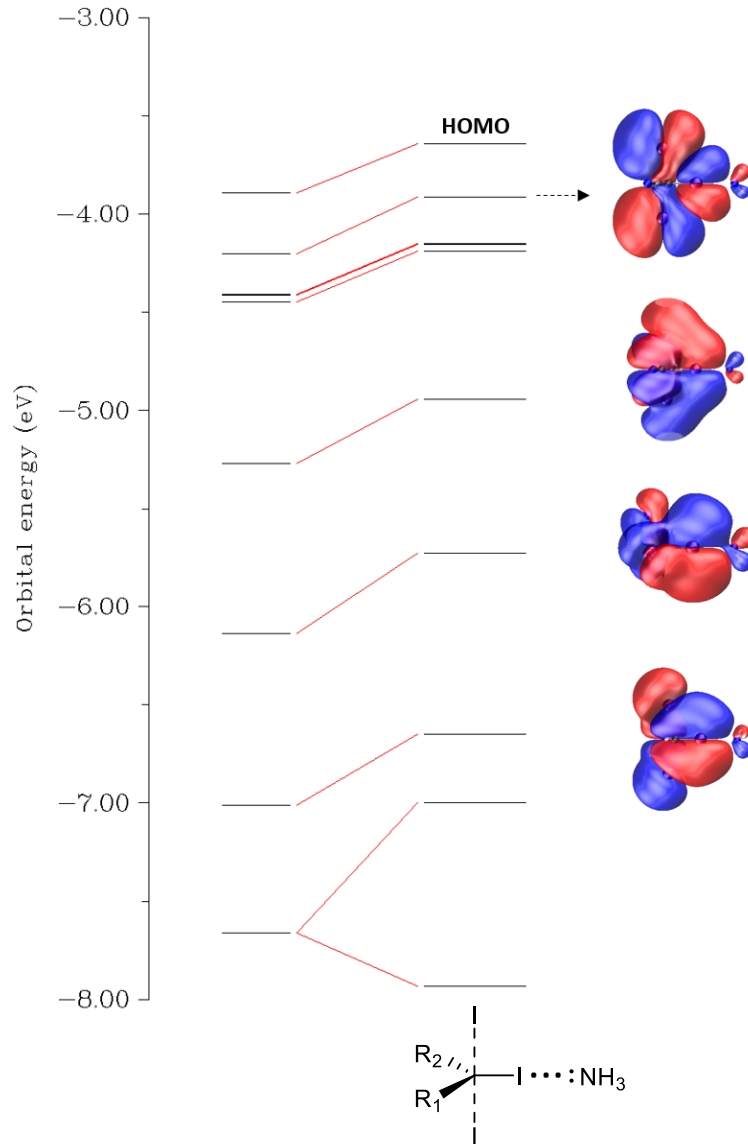
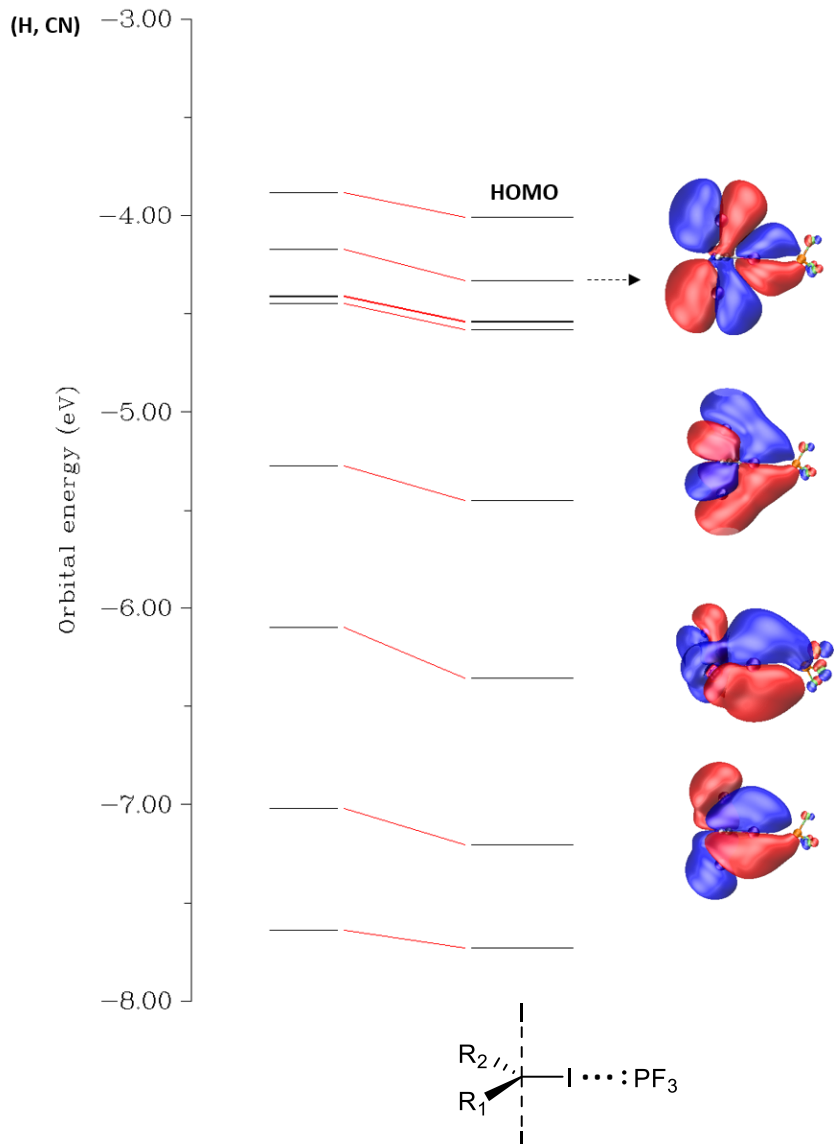


Figure S18. π -type molecular orbitals (MOs) on the isolated diiodomethane that would be involved in backbonding interactions should one be available. The positions of each MO are indicated in the legend after the MO figures. The MOs are visualized at an isosurface value of 0.002.

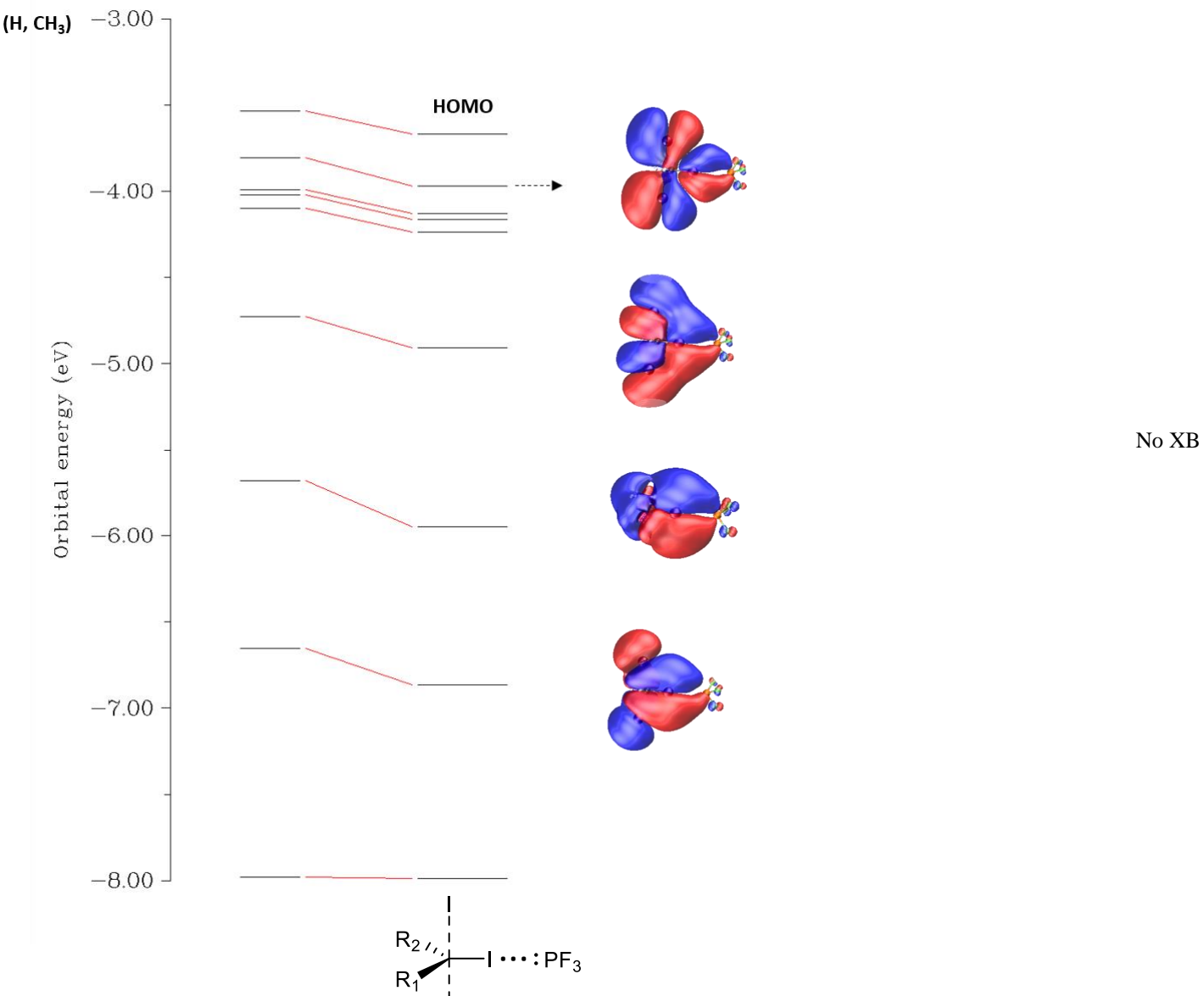


Figure S19. π -type molecular orbitals (MOs) on the isolated diiodomethane that would be involved in backbonding interactions should one be available. The positions of each MO are indicated in the legend after the MO figures. The MOs are visualized at an isosurface value of 0.002.

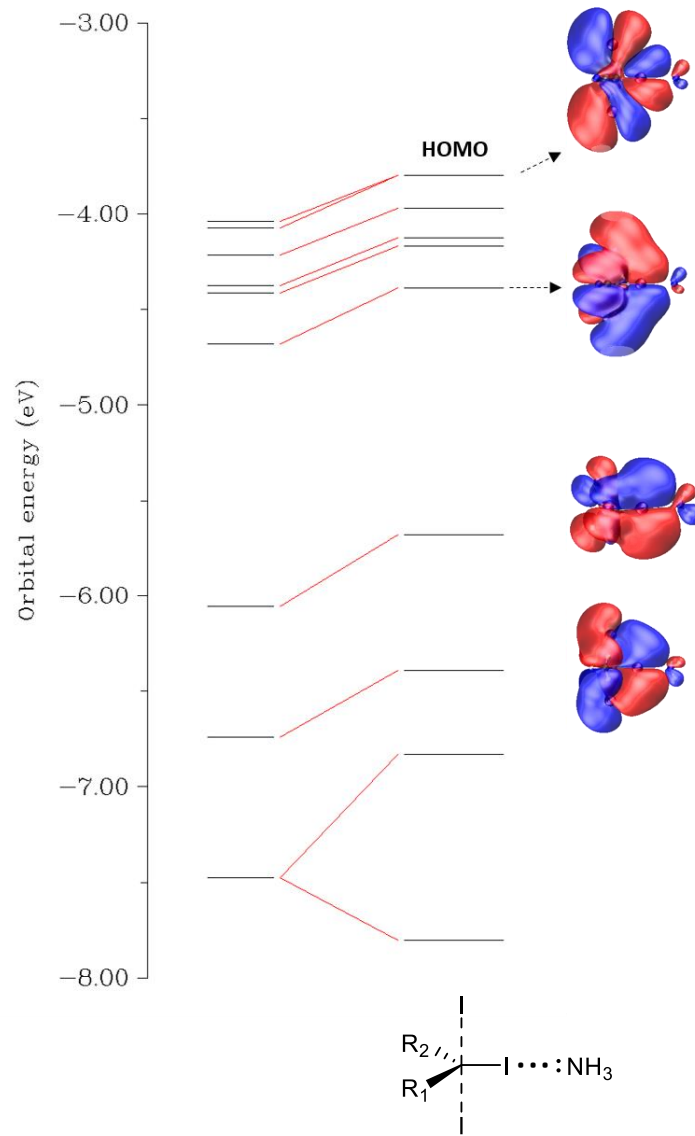
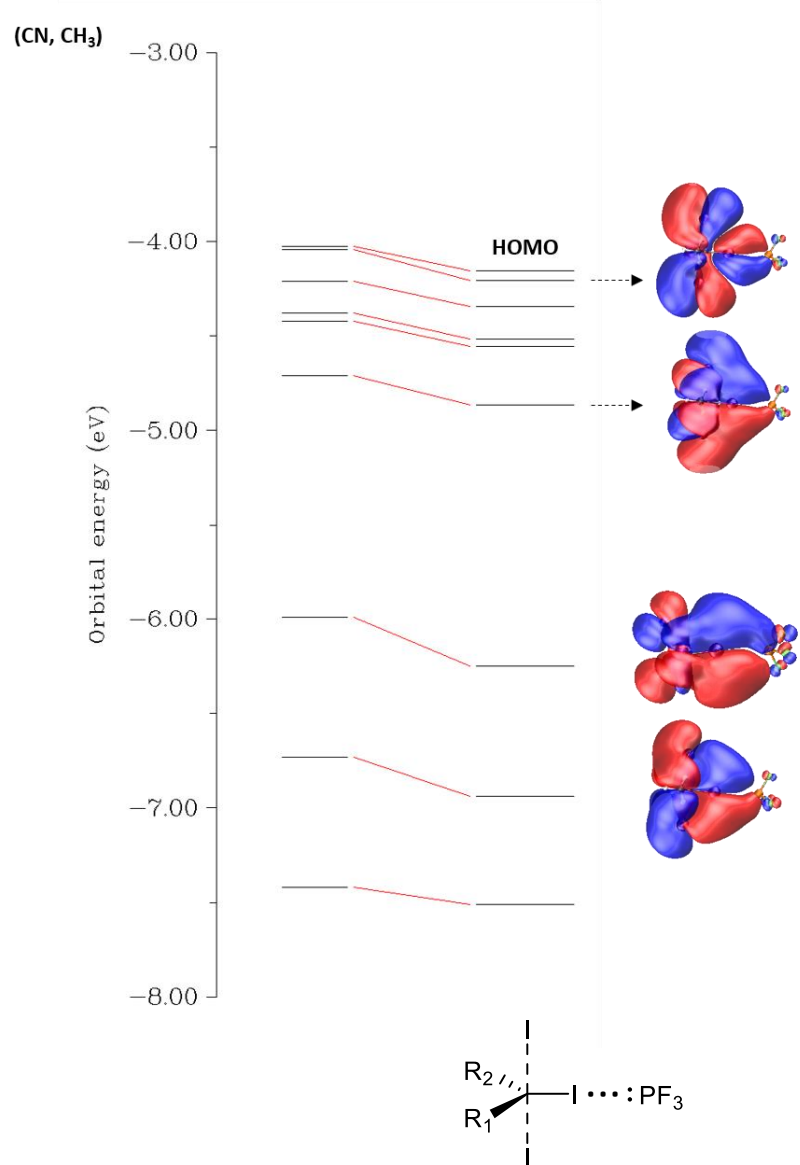


Figure S20. π -type molecular orbitals (MOs) on the isolated diiodomethane that would be involved in backbonding interactions should one be available. The positions of each MO are indicated in the legend after the MO figures. The MOs are visualized at an isosurface value of 0.002.

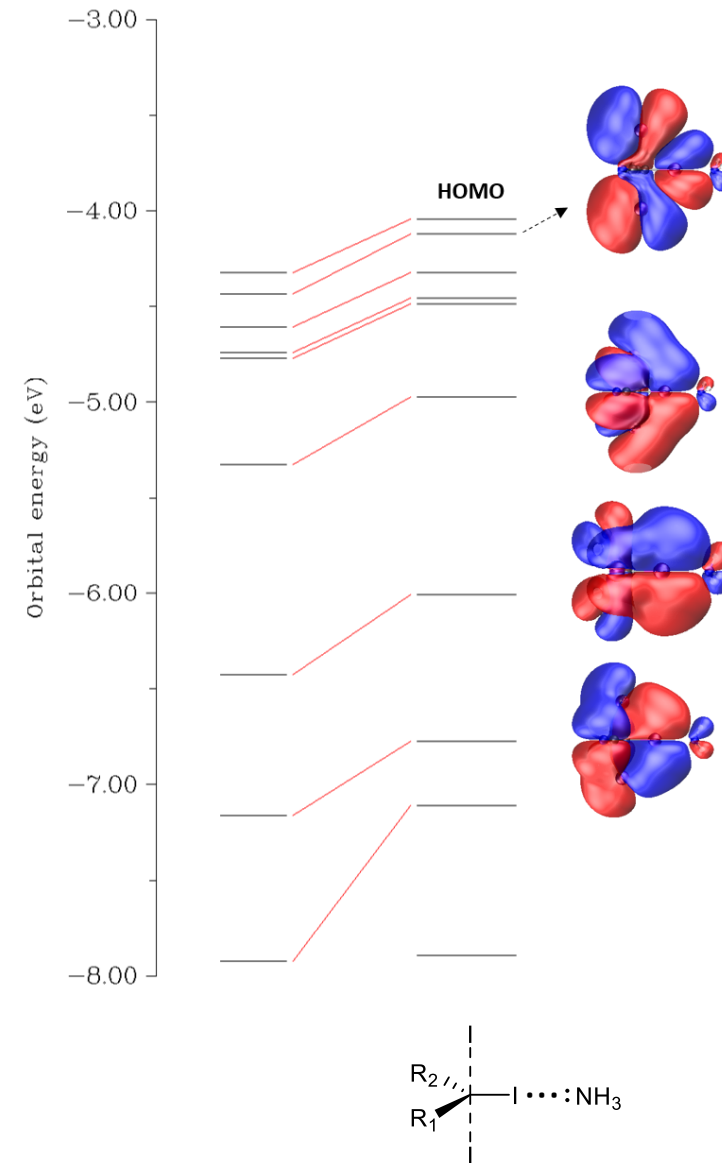
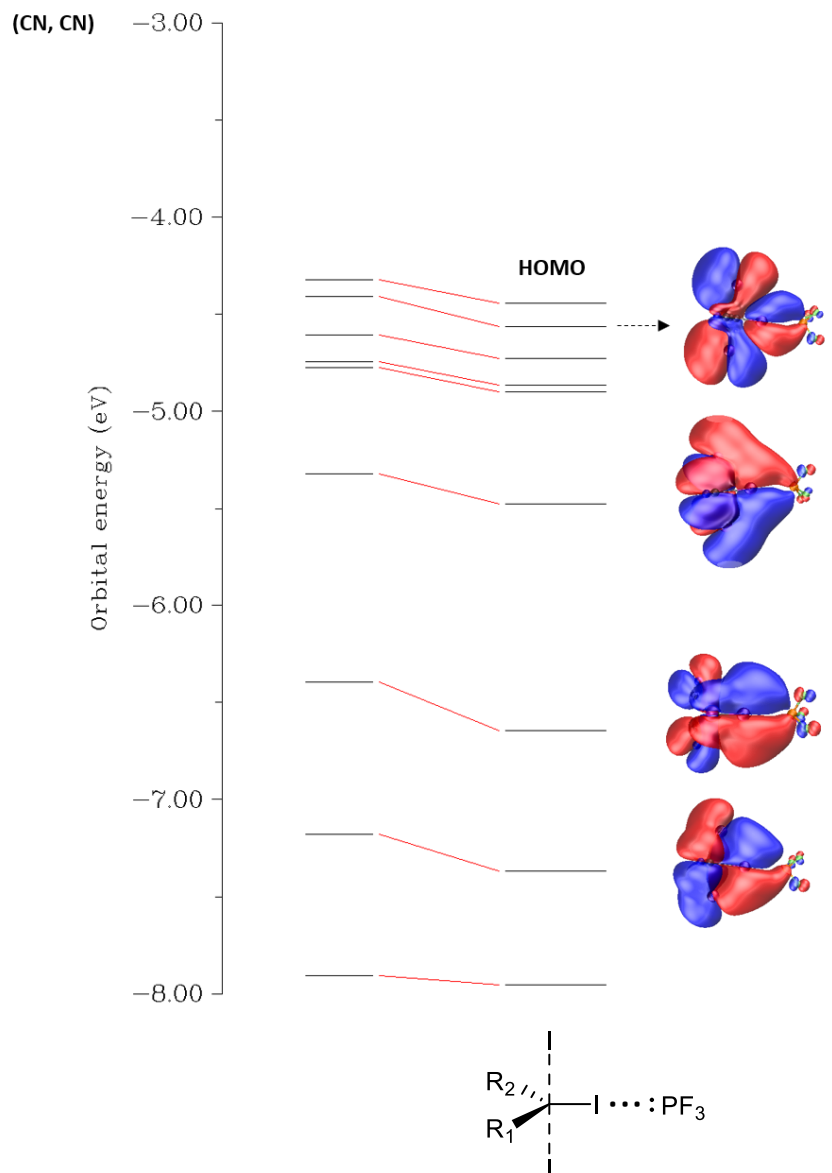


Figure S21. π -type molecular orbitals (MOs) on the isolated diiodomethane that would be involved in backbonding interactions should one be available. The positions of each MO are indicated in the legend after the MO figures. The MOs are visualized at an isosurface value of 0.002.

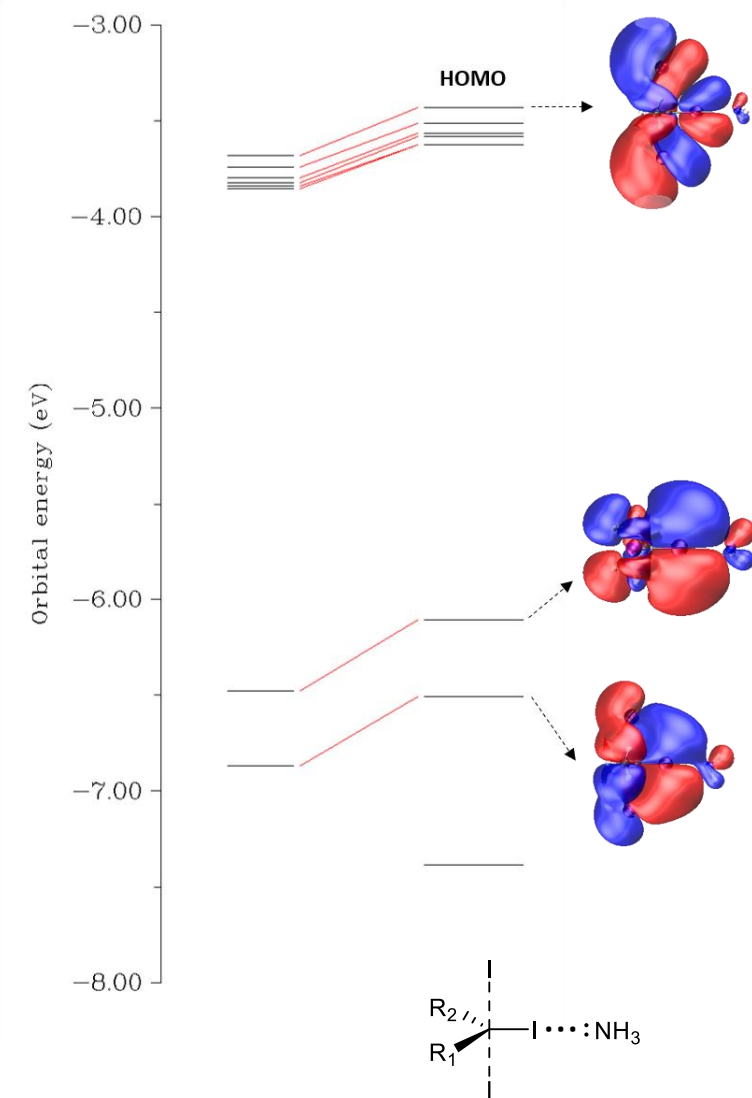
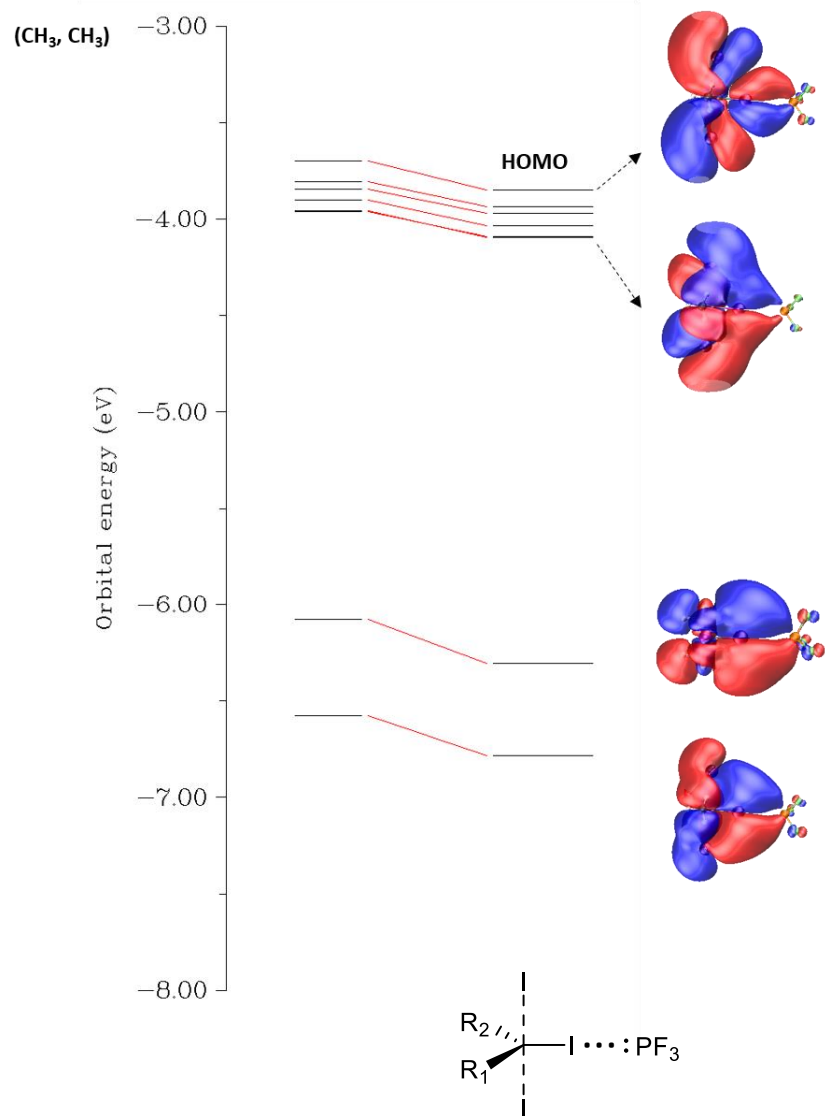


Figure S22. π -type molecular orbitals (MOs) on the isolated diiodomethane that would be involved in backbonding interactions should one be available. The positions of each MO are indicated in the legend after the MO figures. The MOs are visualized at an isosurface value of 0.002.

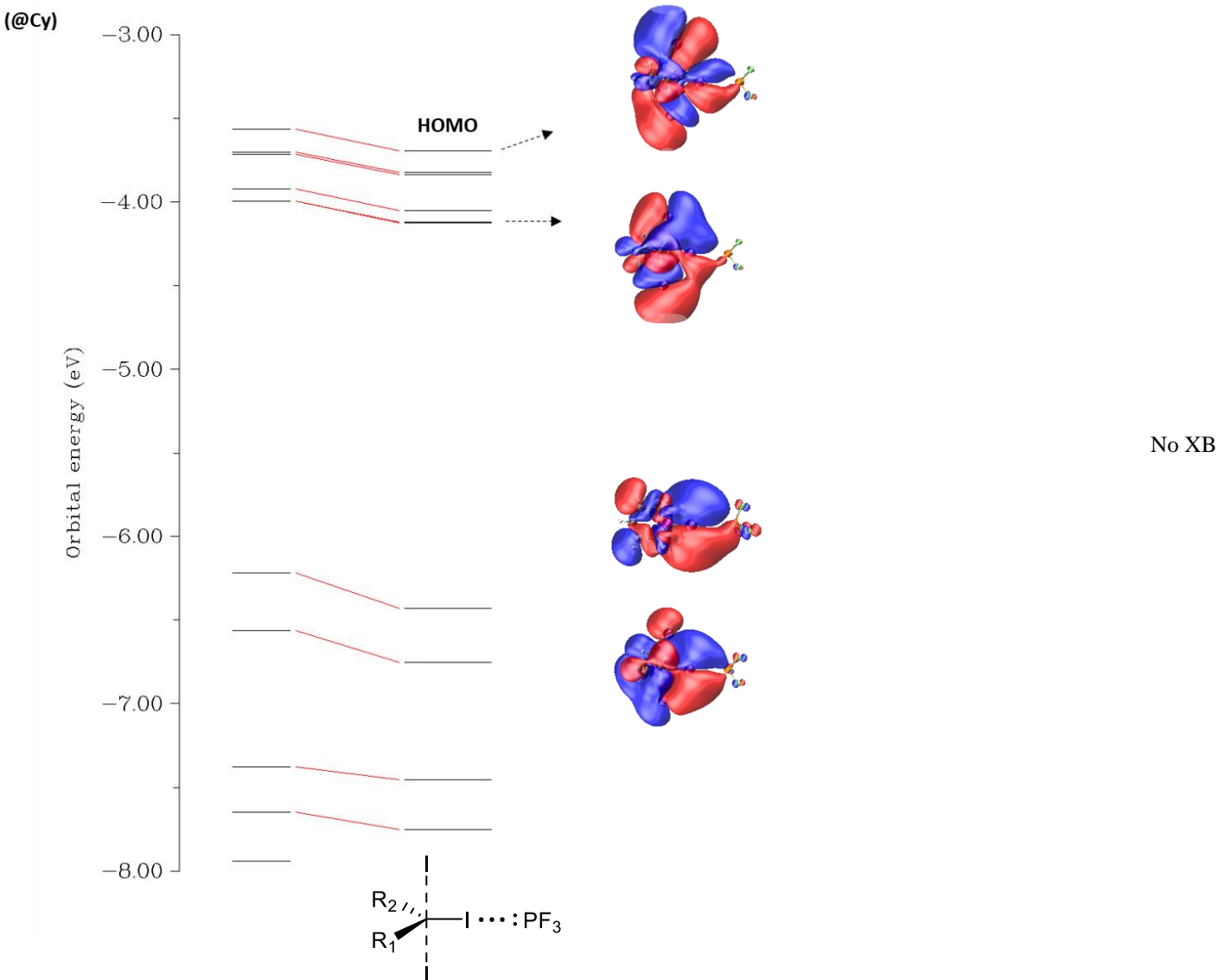
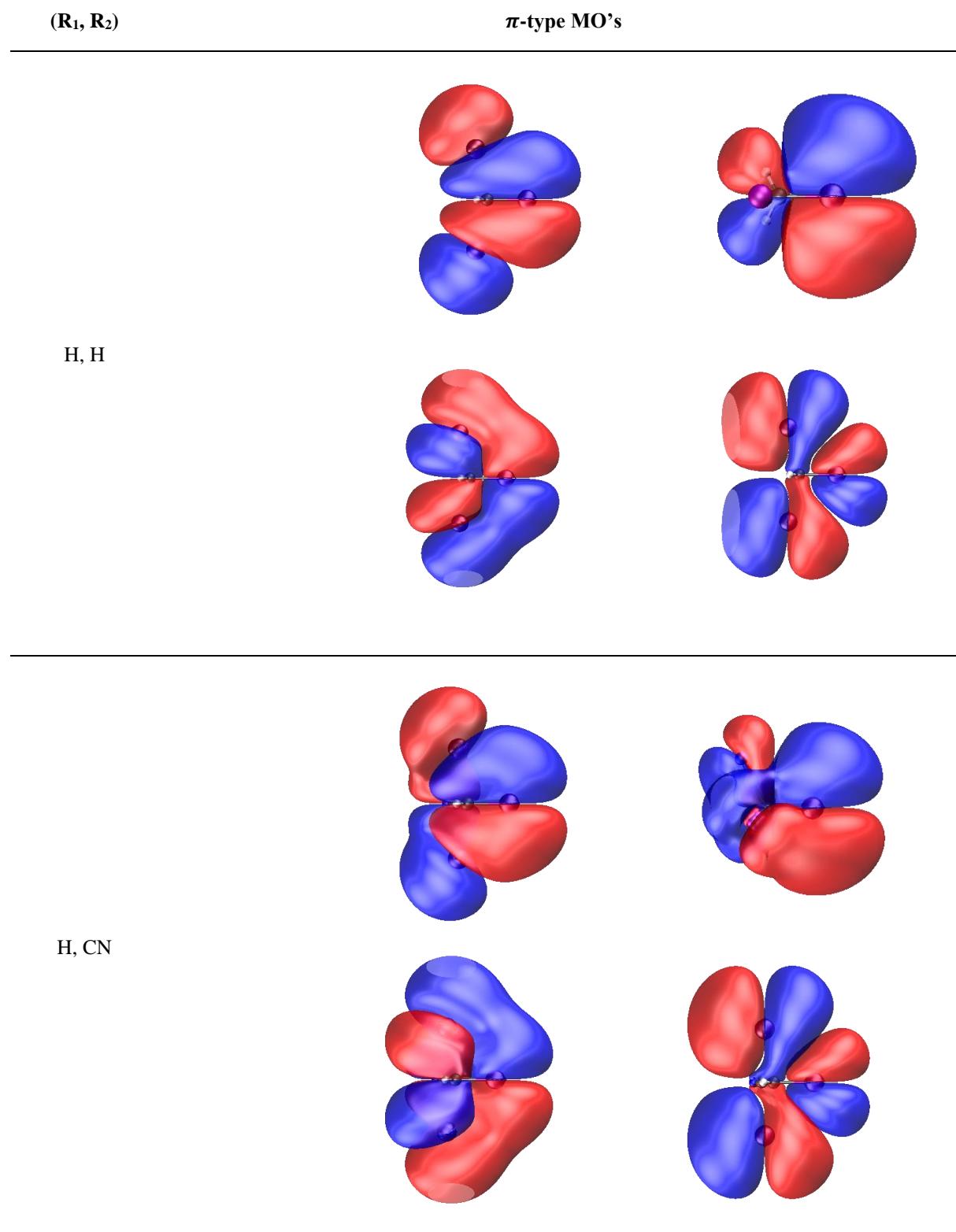
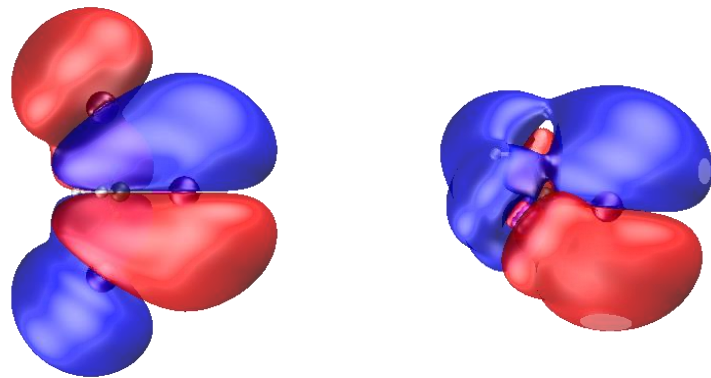


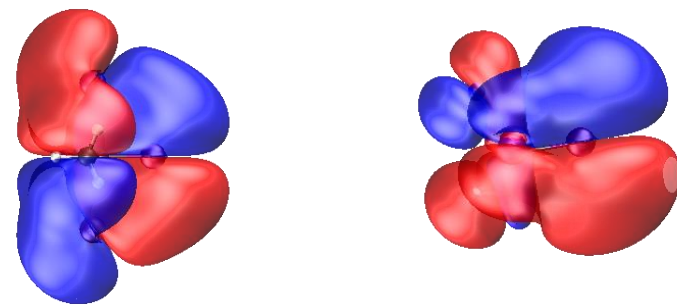
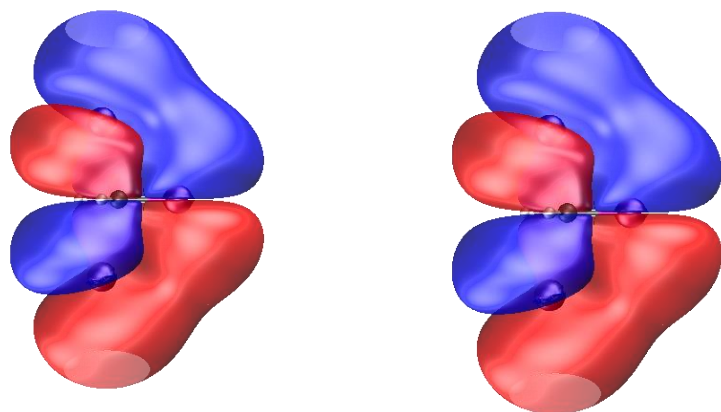
Figure S23. π -type molecular orbitals (MOs) on the isolated diiodomethane that would be involved in backbonding interactions should one be available. The positions of each MO are indicated in the legend after the MO figures. The MOs are visualized at an isosurface value of 0.002.

3.4.2 Isolated diiodomethanes without XB (M06-2X/def2-TZVP)

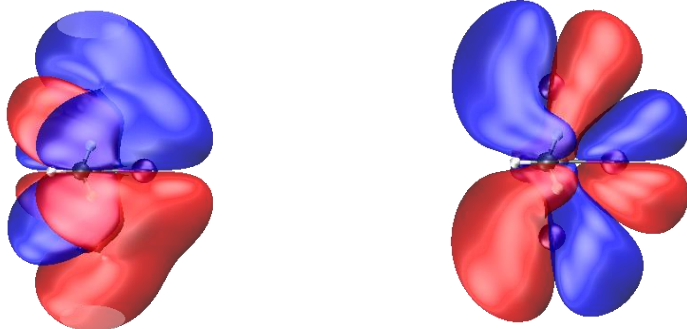


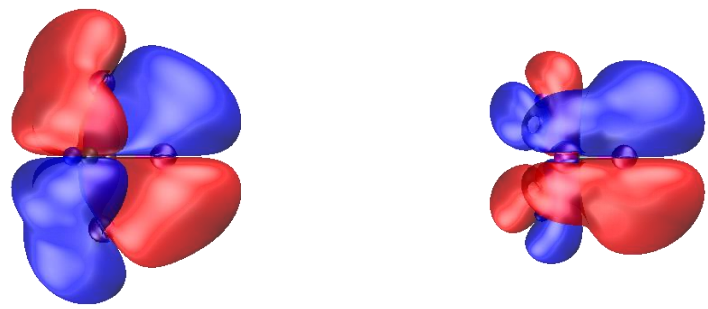


H, CH₃

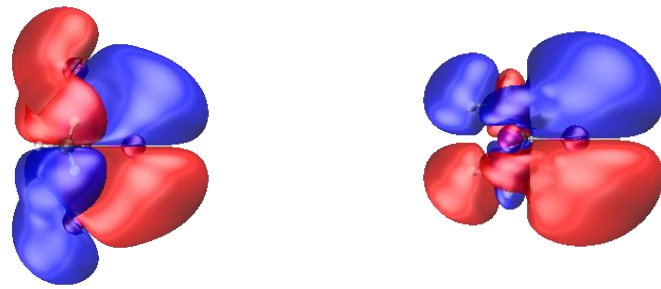
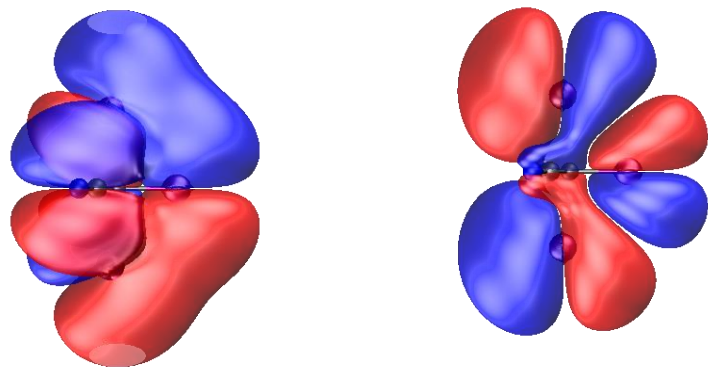


CN, CH₃

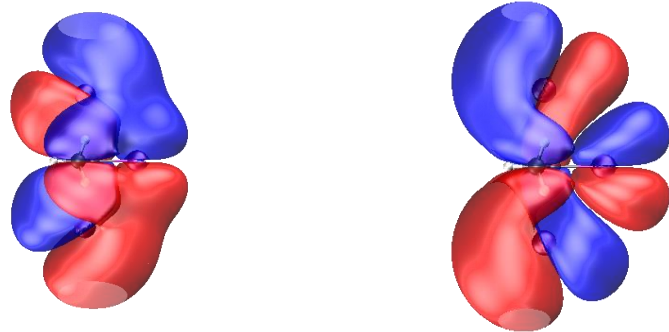


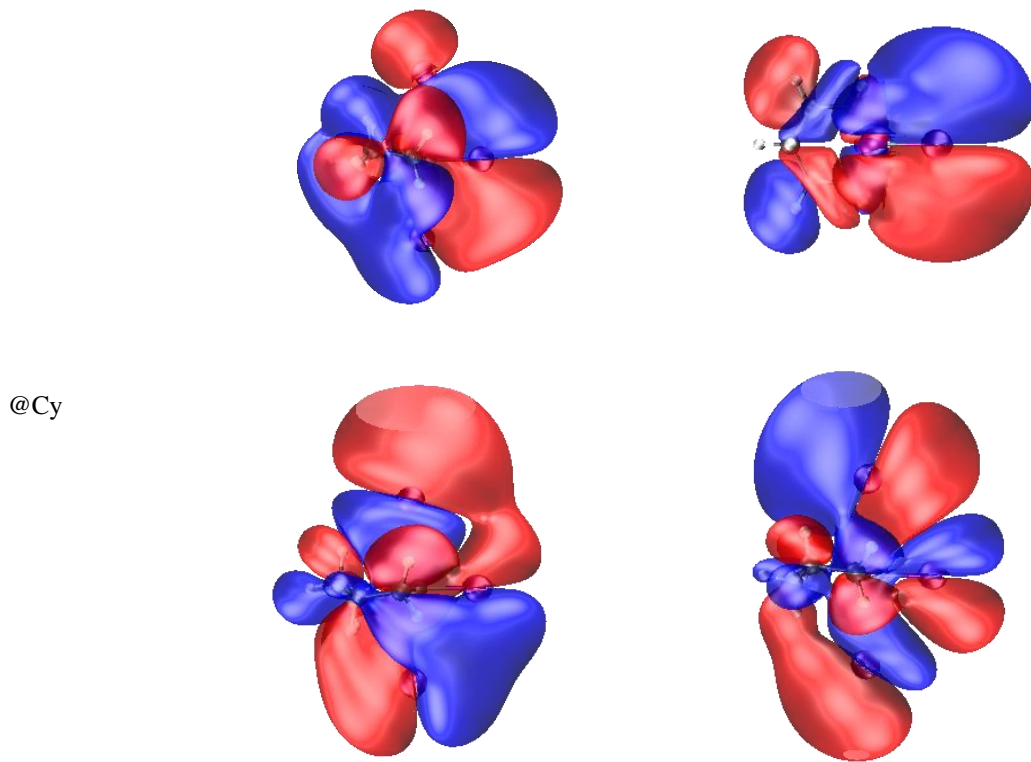


CN, CN



CH₃, CH₃





Legend for

(H, H),

HOMO - 7

HOMO - 6

(H, CN),

HOMO - 5

HOMO - 1

(H, CH₃),

(CH₃, CH₃),

(CN, CN)

Legend for

(CN, CH₃),

HOMO - 7

HOMO - 6

(@Cy)

HOMO - 4

HOMO

Figure S24. π -type molecular orbitals (MOs) on the isolated diiodomethane that would be involved in backbonding interactions should one be available. The positions of each MO are indicated in the legend after the MO figures. The MOs are visualized at an isosurface value of 0.002.

3.5 Gaussian-broadened TDOS for all sets of substituents

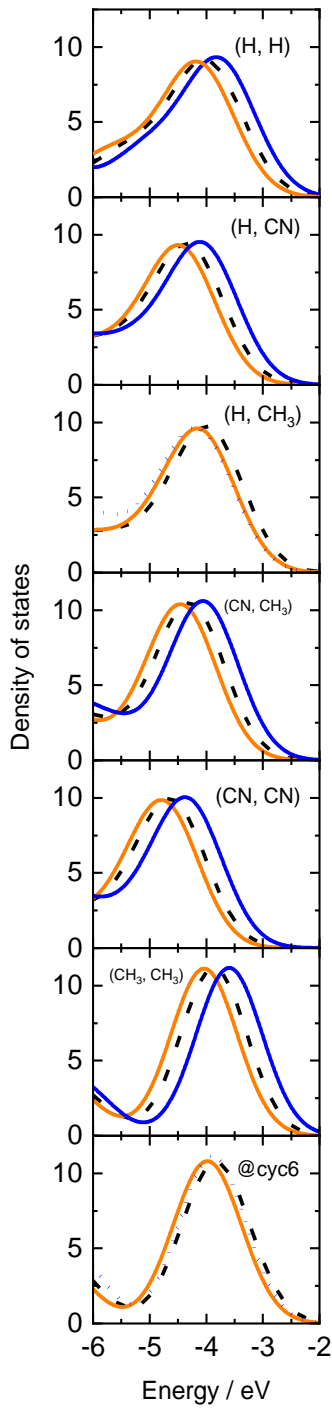


Figure S25. Gaussian-broadened density of states around the HOMO for PF₃ as the electron donor (orange), NH₃ as the electron donor (blue), and no XB (dashed black line), for all substituents. The dotted blue line refers to cases with no XB in the transition state for NH₃.

4. Tables

4.1 Data for $\Delta H_{\text{XB}}^0[\text{GS}]$ and $\Delta H_{\text{XB}}^0[\text{TS}]$

Table S1. $\Delta H_{\text{XB}}^0[\text{GS}]$ and $\Delta H_{\text{XB}}^0[\text{TS}]$ data for CO, PF₃, and NH₃. Units: kJ mol⁻¹

$(\mathbf{R}_1, \mathbf{R}_2)$	CO		PF ₃		NH ₃	
	$\Delta H_{\text{XB}}^0[\text{GS}]$	$\Delta H_{\text{XB}}^0[\text{TS}]$	$\Delta H_{\text{XB}}^0[\text{GS}]$	$\Delta H_{\text{XB}}^0[\text{TS}]$	$\Delta H_{\text{XB}}^0[\text{GS}]$	$\Delta H_{\text{XB}}^0[\text{TS}]$
H, H	-2.454842	-5.888996	0.764020	-10.465242	-20.505153	-3.021950
H, CN	-4.893931	-2.630751	1.743332	-9.323149	-28.851616	-10.360222
H, CH ₃	-1.879858	-5.610693	0.464713	-10.265704	-15.902652	-20.166463
CN, CH ₃	-3.948752	-7.264758	1.509662	-10.011030	-26.176232	-9.349404
CN, CN	-7.422288	-4.321573	2.181790	-9.010715	-40.894783	-17.231155
CH ₃ , CH ₃	-1.488658	-1.622559	0.144402	-7.897503	-14.516388	-9.724851
@Cy	-1.210355	-2.116153	-0.107645	-7.532559	-13.912523	-21.691879

4.2 Raw thermochemical data for GS and TS structures

Table S2. Raw enthalpy data. Units: atomic units (a.u.)

(R ₁ , R ₂)	CO		PF ₃		NH ₃		no XB	
	GS	TS	GS	TS	GS	TS	GS	TS
H, H	-743.766231	-1039.475884	-1271.343135	-1567.055757	-686.980211	-982.681897	-630.479976	-926.188321
H, CN	-835.982925	-1131.694476	-1363.558527	-1659.275155	-779.199155	-1074.904525	-722.695741	-1018.408154
H, CH ₃	-783.035939	-1078.740457	-1310.613176	-1606.32036	-726.248385	-1021.953106	-669.749903	-965.453000
CN, CH ₃	-875.253199	-1170.952946	-1402.829250	-1698.532122	-818.46877	-1114.160845	-761.966375	-1057.664859
CN, CN	-928.190128	-1223.904412	-1455.764600	-1751.484328	-871.409982	-1167.116434	-814.901981	-1110.617446
CH ₃ , CH ₃	-822.305994	-1117.994412	-1349.883502	-1645.574932	-765.518061	-1061.204603	-709.020107	-1004.708474
@Cy	-938.937772	-1234.626803	-1466.515482	-1762.206996	-882.149715	-1177.841364	-825.651991	-1121.340677

Table S3. Raw entropy data. Units: cal mol⁻¹ K⁻¹

(R ₁ , R ₂)	CO		PF ₃		NH ₃		no XB	
	GS	TS	GS	TS	GS	TS	GS	TS
H, H	103.969	106.346	119.662	136.727	92.521	118.163	75.327	91.892
H, CN	112.509	131.684	129.193	143.486	105.413	124.363	84.785	100.325
H, CH ₃	110.736	112.775	125.212	142.142	104.154	120.474	81.772	98.394
CN, CH ₃	118.348	119.532	134.502	149.801	115.568	130.227	90.613	106.422
CN, CN	119.083	135.072	136.158	150.207	118.213	129.436	93.898	108.057
CH ₃ , CH ₃	118.350	140.207	133.057	152.408	109.579	133.248	87.284	107.903
@Cy	104.964	145.440	140.619	158.213	119.144	139.271	96.108	115.149

Table S4. Raw Gibbs energy data. Units: a.u.

(R ₁ , R ₂)	CO		PF ₃		NH ₃		no XB	
	GS	TS	GS	TS	GS	TS	GS	TS
H, H	-743.815630	-1039.526413	-1271.399990	-1567.120720	-687.024170	-982.738040	-630.515766	-926.231982
H, CN	-836.036382	-1131.757043	-1363.619911	-1659.343330	-779.24924	-1074.963614	-722.736025	-1018.455821
H, CH ₃	-783.088553	-1078.794040	-1310.672669	-1606.387896	-726.297872	-1022.010347	-669.788755	-965.499750
CN, CH ₃	-875.309430	-1171.009739	-1402.893156	-1698.603297	-818.523681	-1114.222720	-762.009428	-1057.715424
CN, CN	-928.246708	-1223.968589	-1455.829293	-1751.555696	-871.466149	-1167.177933	-814.946595	-1110.668788
CH ₃ , CH ₃	-822.362226	-1118.061028	-1349.946722	-1645.647346	-765.5701	-1061.267914	-709.061579	-1004.759742
@Cy	-938.997333	-1234.695906	-1466.582295	-1762.282168	-882.206324	-1177.907536	-825.697655	-1121.395388

4.3 Geometric and other data relevant for XB for GS and TS

Table S5. Geometric data, information about the presence of XB, and information about imaginary frequencies in the GS with CO as the electron donor.

(R ₁ , R ₂)	XB present?	no imag freq?	r _{C[E]...Nu} (Å)	r _{C[E]...LG} (Å)	r _{C[E]-I[XB]} (Å)	XB angle (deg)
H, H	TRUE	TRUE	2.141	2.138	3.439	179.761
H, CN	TRUE	TRUE	2.157	2.155	3.320	178.152
H, CH ₃	TRUE	TRUE	2.163	2.159	3.473	178.735
CN, CH ₃	TRUE	TRUE	2.178	2.175	3.349	178.359
CN, CN	TRUE	TRUE	2.177	2.18	3.228	179.647
CH ₃ , CH ₃	TRUE	TRUE	2.187	2.182	3.495	177.658
@Cy	TRUE	TRUE	2.198	2.181	3.499	179.108

Table S6. Geometric data and information about the presence of XB and imaginary frequencies in the TS with CO as the electron donor.

(R ₁ , R ₂)	XB present?	imag freq (cm ⁻¹)	r _{C[E]...Nu} (Å)	r _{C[E]...LG} (Å)	r _{C[E]-I[XB]} (Å)	r _{C[=O]...I[XB]} (Å)	XB angle (deg)
H, H	TRUE	-421.3446, -12, -7	2.719	2.719	2.095	3.450	179.676
H, CN	TRUE	-382.9649	2.754	2.755	2.108	3.346	178.956
H, CH ₃	TRUE	-424.1913, -9, -4	2.822	2.821	2.103	3.479	179.607
CN, CH ₃	TRUE	-333.6183, -4, -2	2.870	2.870	2.124	3.361	178.454
CN, CN	TRUE	-288.4404	2.795	2.794	2.133	3.267	179.890
CH ₃ , CH ₃	TRUE	-322.8353	3.191	3.191	2.086	3.456	178.718
@Cy	TRUE	-280.7829	3.171	3.399	2.081	3.437	173.242

Table S7. Geometric data, information about the presence of XB, and information about imaginary frequencies in the GS with PF₃ as the electron donor.

(R ₁ , R ₂)	XB present?	no imag freq?	r _{C[E]...Nu} (Å)	r _{C[E]...LG} (Å)	r _{C[E]-I[XB]} (Å)	XB angle (deg)
H, H	TRUE	TRUE	2.137	2.141	3.757	176.372
H, CN	TRUE	TRUE	2.153	2.158	3.713	173.923
H, CH ₃	TRUE	TRUE	2.159	2.163	3.772	175.323
CN, CH ₃	TRUE	TRUE	2.175	2.179	3.726	177.514
CN, CN	TRUE	TRUE	2.176	2.182	3.641	177.686
CH ₃ , CH ₃	TRUE	TRUE	2.184	2.188	3.782	176.771
@Cy	TRUE	TRUE	2.194	2.188	3.783	177.370

Table S8. Geometric data and information about the presence of XB and imaginary frequencies in the TS with PF₃ as the electron donor.

(R ₁ , R ₂)	XB present?	imag freq (cm ⁻¹)	r _{C[E]...Nu} (Å)	r _{C[E]...LG} (Å)	r _{C[E]-I[XB]} (Å)	r _{P...I[XB]} (Å)	XB angle (deg)
H, H	TRUE	-420.5229	2.708	2.708	2.098	3.672	176.425
H, CN	TRUE	-385.7638	2.746	2.747	2.109	3.639	175.623
H, CH ₃	TRUE	-425.3031	2.804	2.804	2.108	3.691	176.376
CN, CH ₃	TRUE	-334.1708	2.857	2.858	2.127	3.640	173.353
CN, CN	TRUE	-291.0045	2.788	2.790	2.133	3.581	174.816
CH ₃ , CH ₃	TRUE	-356.4671	3.120	3.119	2.100	3.718	177.298
@Cy	TRUE	-307.2974	3.143	3.326	2.089	3.723	173.068

Table S9. Geometric data, information about the presence of XB, and information about imaginary frequencies in the GS with NH₃ as the electron donor.

(R ₁ , R ₂)	XB present?	no imag freq?	r _{C[E]...Nu} (Å)	r _{C[E]...LG} (Å)	r _{C[E]-I[XB]} (Å)	XB angle (deg)
H, H	TRUE	-8.938	2.147	2.143	3.048	179.061
H, CN	TRUE	TRUE	2.161	2.168	2.909	179.418
H, CH ₃	TRUE	TRUE	2.169	2.159	3.071	179.076
CN, CH ₃	TRUE	TRUE	2.182	2.183	2.933	179.026
CN, CN	TRUE	TRUE	2.179	2.209	2.759	179.681
CH ₃ , CH ₃	TRUE	TRUE	2.195	2.179	3.086	179.473
@Cy	TRUE	TRUE	2.205	2.179	3.091	179.420

Table S10. Geometric data and information about the presence of XB and imaginary frequencies in the TS with NH₃ as the electron donor.

(R ₁ , R ₂)	XB present?	imag freq (cm ⁻¹)	r _{C[E]...Nu} (Å)	r _{C[E]...LG} (Å)	r _{C[E]-I[XB]} (Å)	r _{N...I[XB]} (Å)	XB angle (deg)
H, H	TRUE	-406.2018	2.731	2.731	2.098	3.139	179.068
H, CN	TRUE	-369.9847	2.763	2.764	2.117	3.017	179.863
H, CH ₃	FALSE	-429.9851	2.802	2.829	2.104	no XB	no XB
CN, CH ₃	TRUE	-327.1343	2.891	2.890	2.128	3.030	178.829
CN, CN	TRUE	-277.9155	2.800	2.801	2.150	2.911	179.970
CH ₃ , CH ₃	TRUE	-274.7015	3.279	3.289	2.078	3.077	176.363
@Cy	FALSE	-260.2340	3.237	3.433	2.067	no XB	no XB

Table S11. Geometric data for the diiodomethanes in the GS without XB. Labels 1 and 2 are arbitrarily chosen for the two iodine atoms.

$(\mathbf{R}_1, \mathbf{R}_2)$	no imag freq?	$r_{\text{C}[\text{E}] \cdots \text{I}[1]} (\text{\AA})$	$r_{\text{C}[\text{E}] - \text{I}[2]} (\text{\AA})$
H, H	TRUE	2.139	2.139
H, CN	TRUE	2.155	2.154
H, CH ₃	TRUE	2.161	2.160
CN, CH ₃	TRUE	2.176	2.176
CN, CN	TRUE	2.177	2.177
CH ₃ , CH ₃	TRUE	2.185	2.185
@Cy	TRUE	2.195	2.186

Table S12. Geometric data and imaginary frequencies for the diiodomethanes in the TS without XB. Here, I[XB] is labelled as such even there is no XB actually present as it would be the halogen-bonded iodine should there be XB.

$(\mathbf{R}_1, \mathbf{R}_2)$	imag freq (cm^{-1})	$r_{\text{C}[\text{E}] \cdots \text{Nu}} (\text{\AA})$	$r_{\text{C}[\text{E}] \cdots \text{LG}} (\text{\AA})$	$r_{\text{C}[\text{E}] - \text{I}[XB]} (\text{\AA})$
H, H	-428.0360	2.717	2.717	2.095
H, CN	-391.0824	2.754	2.754	2.106
H, CH ₃	-428.8063	2.82	2.821	2.103
CN, CH ₃	-340.7992	2.868	2.871	2.123
CN, CN	-295.7395	2.794	2.795	2.130
CH ₃ , CH ₃	-335.6470	3.177	3.175	2.088
@Cy	-291.2538	3.169	3.386	2.081

4.4 NPA raw data

Table S13. NPA charges on select atoms for the TS with CO as the electron donor.

(R ₁ , R ₂)	NPA _{C[E]}	NPA _{Nu}	NPA _{LG}	NPA _{I[XB]}	NPA _{C=O}	NPA _O
H, H	-0.66795	-0.55403	-0.55389	0.18974	0.53732	-0.53348
H, CN	-0.57319	-0.47733	-0.47803	0.26330	0.53483	-0.52696
H, CH ₃	-0.35931	-0.59726	-0.59686	0.19502	0.53828	-0.53355
CN, CH ₃	-0.27992	-0.49519	-0.49519	0.26331	0.53657	-0.52811
CN, CN	-0.47165	-0.38135	-0.38132	0.31142	0.53417	-0.52139
CH ₃ , CH ₃	0.08502	-0.75912	-0.75889	0.28520	0.53425	-0.52699
@Cy	0.15676	-0.74233	-0.83692	0.31057	0.53293	-0.52507

Table S14. NPA charges on select atoms for the TS with PF₃ as the electron donor.

(R ₁ , R ₂)	NPA _{C[E]}	NPA _{Nu}	NPA _{LG}	NPA _{I[XB]}	NPA _P	NPA _{3F}
H, H	-0.67245	-0.54132	-0.54146	0.15608	1.79552	-1.78528
H, CN	-0.57303	-0.46623	-0.46643	0.22754	1.79376	-1.77919
H, CH ₃	-0.36674	-0.58122	-0.58079	0.15640	1.79705	-1.78571
CN, CH ₃	-0.28236	-0.48036	-0.48085	0.22408	1.79641	-1.78104
CN, CN	-0.46856	-0.37099	-0.37249	0.27467	1.79402	-1.77418
CH ₃ , CH ₃	0.05202	-0.71268	-0.71210	0.22298	1.79541	-1.78104
@Cy	0.14402	-0.72002	-0.80100	0.25981	1.79449	-1.77943

Table S15. NPA charges on select atoms for the TS with NH₃ as the electron donor. Entries in red indicate that no XB is present for that set.

(R ₁ , R ₂)	NPA _{C[E]}	NPA _{Nu}	NPA _{LG}	NPA _{I[XB]}	NPA _N	NPA _{3H}
H, H	-0.66621	-0.57043	-0.57074	0.21785	-1.12564	1.14436
H, CN	-0.57476	-0.49516	-0.49536	0.28852	-1.12627	1.15757
H, CH ₃	-0.35506	-0.57976	-0.59623	0.18369	-1.14465	1.13863
CN, CH ₃	-0.27558	-0.51977	-0.51930	0.29585	-1.12603	1.15674
CN, CN	-0.47394	-0.39968	-0.39993	0.33177	-1.12366	1.17148
CH ₃ , CH ₃	0.12485	-0.81833	-0.81592	0.34652	-1.13081	1.15623
@Cy	0.17420	-0.77839	-0.85555	0.35532	-1.15534	1.14598

Table S16. NPA charges on select atoms for the TS in the absence of XB.

(R ₁ , R ₂)	NPA _{C[E]}	NPA _{Nu}	NPA _{LG}	NPA _{I[XB]}	Electron donor	NPA _Y	NPA _Z
H, H	-0.66185	-0.55076	-0.55053	0.17661	CO	0.50821	-0.50821
H, CN	-0.56551	-0.47375	-0.47394	0.25108	PF ₃	1.77105	-1.77105
H, CH ₃	-0.35400	-0.59337	-0.59413	0.18350	NH ₃	-1.12195	1.12194
CN, CH ₃	-0.27297	-0.48933	-0.49224	0.25199			
CN, CN	-0.46181	-0.37605	-0.37681	0.29963			
CH ₃ , CH ₃	0.08166	-0.74828	-0.74766	0.27126			
@Cy	0.15895	-0.73870	-0.82978	0.30137			

Table S17. NPA charges on groups of the electron donor in the absence of XB.

4.5 Expanded tables for CDA

Table S18. Expanded summary data table for charge decomposition analysis results (see section 2 for description of terms). Note that values are listed in their original form as opposed to 10^{-3} e⁻ as shown in the main text. See Section 2 of this document for a description of terms.

(R ₁ , R ₂)	π orbitals					σ orbital
	$\sum \rho_{\pi}^D$	$\sum \rho_{\pi}^A$	$\rho_{\pi}^D[\text{frag}]$	$\sum \rho_{\pi}^A[\text{frag}]$	$\frac{\sum \rho_{\pi}^A[\text{frag}]}{\sum \rho_{\pi}^A}$ (%)	ρ_{σ}^D
H, H	0.00003	0.00944	0	0.00710	75.17%	0.013435
H, CN	0.00008	0.00938	0	0.00582	62.07%	0.018280
H, CH ₃	0.00002	0.00859	0	0.00681	79.36%	0.018317
CN, CH ₃	0.00008	0.00949	0	0.00646	68.10%	0.011938
CN, CN	0.00010	0.01043	0	0.00906	86.83%	0.027048
CH ₃ , CH ₃	0.00001	0.00700	0	0.00562	80.38%	0.019357
@Cy	0.00005	0.00616	0	0.00508	82.49%	0.018312

Table S19. Raw and calculated data from charge decomposition analysis of the π interaction. Values are listed in their original form as opposed to 10^{-3} e⁻ as shown in the main text. See Section 2 of this document for a description of terms.

complex π MO	ρ_{π}^D	ρ_{π}^A	$\Sigma\rho_{\pi}^D$	$\Sigma\rho_{\pi}^A$	fragment π MOs (PF ₃ /CR ₂ I ₂)	$\rho_{\pi}^D[\text{frag}]$	$\rho_{\pi}^A[\text{frag}]$	$\Sigma\rho_{\pi}^A[\text{frag}]$	$\frac{\rho_{\pi}^A[\text{frag}]}{\rho_{\pi}^A}$ (%)	$\frac{\Sigma\rho_{\pi}^A[\text{frag}]}{\Sigma\rho_{\pi}^A}$ (%)
H, H	56	0.000017	0.001148		22/35	0	0.000735		64.02439024	
	57	0.000007	0.004134	0.000031	23/36	0	0.003043	0.007096	73.60909531	
	58	0.000004	0.002645	0.009440	22/37	0	0.002065		78.07183365	75.17%
	62	0.000003	0.001513		22/41	0	0.001253		82.81559815	
H, CN	62	0.000010	0.001542		23/41	0	0.000827		53.63164721	
	63	0.000066	0.004269	0.000080	22/42	0	0.002677	0.005822	62.70789412	
	64	0.000002	0.002029	0.009380	23/43	0	0.001296		63.87382947	62.07%
	68	0.000002	0.00154		23/47	0	0.001022		66.36363636	
H, CH ₃	60	0.000018	0.001701		22/39	0	0.001203		70.72310406	
	61	-0.000001	0.003746	0.000022	23/40	0	0.002961	0.006813	79.04431393	
	62	0.000002	0.001760	0.008585	22/41	0	0.001458		82.84090909	79.36%
	66	0.000003	0.001378		22/45	0	0.001191		86.42960813	
CN, CH ₃	66	0.000020	0.002132		23/45	0	0.001267		59.42776735	
	67	0.000053	0.004266	0.000078	22/46	0	0.003002	0.006461	70.37037037	
	68	0.000001	0.001371	0.009488	23/47	0	0.000947		69.07366885	68.10%
	72	0.000004	0.001719		23/51	0	0.001245		72.42582897	
CN, CN	68	0.000062	0.002261		22/47	0	0.001795		79.38965060	
	69	0.000017	0.004275	0.000102	23/48	0	0.003583	0.009055	83.8128655	
	70	0.000009	0.001881	0.010428	22/49	0	0.001767		93.93939394	86.83%
	74	0.000014	0.002011		22/53	0	0.001910		94.97762307	
CH ₃ , CH ₃	64	0.000005	0.002192		22/53	0	0.001689		77.05291971	
	65	0.000004	0.003178	0.000010	23/54	0	0.002551	0.005624	80.27061045	
	66	0	0.000451	0.006997	22/46	0	0.000359		79.60088692	80.38%
	71	0.000001	0.001176		22/50	0	0.001025		87.15986395	
@Cy	75	-0.000006	0.002055		22/54	0	0.001697		82.57907543	
	76	0.000050	0.003211	0.000053	23/55	0	0.002607	0.005078	81.18966054	
	77	0	0.000315	0.006156	22/56	0	0.000257		81.58730159	82.49%
	82	0.000009	0.000575		22/61	0	0.000517		89.91304348	

5. Cartesian coordinates and electronic energies of ground state and transition state structures

5.1 Ground state

5.1.1 Ground state, CO as electron donor

(R₁, R₂)	RM062X energy (a. u.)	Cartesian coordinates
H, H	-743.808440224	C 0.00000000 0.00000000 0.00000000 I -2.02086400 -0.69872500 0.00011100 H 0.14809700 0.59567600 0.90385800 I 1.49058600 -1.53727800 0.00008800 H 0.14805300 0.59552600 -0.90396500 C -5.26673600 -1.83616600 0.00007000 O -6.31104000 -2.26028700 0.00005000
H, CN	-836.025600257	C 0.00000000 0.00000000 0.00000000 I 1.41821700 -1.49496200 -0.63652300 C 0.30260800 1.27209900 -0.62726000 N 0.54146600 2.29316600 -1.11817300 I -2.05378800 -0.54551900 -0.35991100 H 0.11507300 0.07901700 1.08509600 C -5.24038000 -1.36123400 -0.81264400 O -6.32795700 -1.62205500 -0.94648000
H, CH ₃	-783.107768665	C 0.00000000 0.00000000 0.00000000 I 1.37630800 -1.62219700 0.38900100 H 0.13959400 0.22851300 -1.06048800 I -2.05593800 -0.63510700 0.17020000 C 0.28797900 1.18495000 0.89845200 H -0.39017400 2.01236200 0.64106800 H 0.14329600 0.92489800 1.95571100 H 1.32710500 1.51534900 0.75295300 C -5.34958700 -1.68079600 0.51552800 O -6.38578200 -2.09162400 0.68388800

CN, CH ₃	-875.325198213	C 0.00000000 0.00000000 0.00000000 I 2.07780800 -0.60204800 -0.22192700 C -0.26258300 1.04855500 -0.97611100 N -0.47774600 1.91178100 -1.71781700 I -1.32953900 -1.66231600 -0.45913900 C -0.25675200 0.48747100 1.42368900 H -0.05478000 -0.32023600 2.13800500 H 0.40338800 1.33991600 1.63934300 H -1.30439800 0.80675800 1.51802700 C 5.30404900 -1.44984900 -0.51680100 O 6.39439300 -1.70485300 -0.64070800
CN, CN	-928.232880752	C 0.00000000 0.00000000 0.00000000 I -1.31270000 -1.73725700 0.00304300 C -0.27084600 0.78296800 1.19841200 N -0.47680400 1.39495100 2.15841800 I 2.10114000 -0.58038500 0.00750000 C -0.26461600 0.77383100 -1.20572500 N -0.46560500 1.37835900 -2.17149200 C 5.21716300 -1.42444400 0.00685100 O 6.30104100 -1.72779400 -0.00744600
CH ₃ , CH ₃	-822.406956995	C 0.00000000 0.00000000 0.00000000 I -2.07017400 -0.68807100 -0.03849100 C 0.23643600 0.77799100 1.28380700 H 0.04296600 0.16690300 2.17397600 H 1.28106600 1.12547700 1.30962800 H -0.43119000 1.65393700 1.30088500 I 1.33040700 -1.73579100 -0.01619500 C 0.26792600 0.82643800 -1.24675200 H 0.09648400 0.25027600 -2.16428900 H -0.39911300 1.70300000 -1.24647700 H 1.31282800 1.17379600 -1.23329900 C -5.42367600 -1.67311700 -0.02747100 O -6.50834200 -1.97496800 0.03173000

@Cy -939.107037622

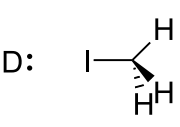
C	0.00000000	0.00000000	0.00000000
C	-0.43472100	-0.73557100	-1.26703900
C	0.00165000	0.00008300	-2.53348100
C	1.49775700	0.32874000	-2.52757000
C	1.89138400	1.09702800	-1.26546100
C	1.49612700	0.32856600	-0.00397100
H	2.07969700	-0.60383900	0.06528400
H	1.72718500	0.91783600	0.89616500
H	2.97331500	1.29683100	-1.26473500
H	1.38603500	2.07939400	-1.26572500
H	2.08146800	-0.60361800	-2.59622500
H	1.72993100	0.91815600	-3.42732100
H	-0.28107500	-0.57583400	-3.42541800
H	-0.57342400	0.94326400	-2.55638000
I	0.40465000	-2.76680100	-1.26655000
I	-2.60796500	-0.92407200	-1.26846300
H	-0.57505900	0.94320800	0.02221400
H	-0.28388500	-0.57595300	0.89154700
C	-6.09827900	-1.17222000	-1.26773500
O	-7.22094500	-1.27649900	-1.26225900

5.1.2 Ground state, PF₃ as electron donor

(R ₁ , R ₂)	RM062X energy (a. u.)	Cartesian coordinates
H, H	-1271.39078276	C 0.00000000 0.00000000 0.00000000 I 2.05505900 0.59867200 -0.05602000 H -0.15427400 -0.55225500 0.92993700 I -1.40915300 1.60658000 -0.04126800 H -0.18333200 -0.62427800 -0.87763900 P 5.71587100 1.44151200 -0.05213800 F 6.73076600 0.32614000 -0.63237700 F 6.45592900 1.65133900 1.36849500 F 6.37840300 2.71010700 -0.80142800
H, CN	-1363.60661743	C 0.00000000 0.00000000 0.00000000 I 1.10921300 -1.74685000 -0.59640200 C 0.44962800 1.16002100 -0.74455900 N 0.80969900 2.09138900 -1.33042900 I -2.13630800 -0.22965200 -0.20223000 H 0.19221600 0.13619300 1.06841500 P -5.74372000 -1.00804800 -0.60828500 F -6.79489500 -0.20795800 -1.53426100 F -6.71742200 -1.20899700 0.66315100 F -5.97451400 -2.46474900 -1.26327800
H, CH ₃	-1310.69044991	C 0.00000000 0.00000000 0.00000000 I -1.30488500 -1.67194300 -0.40150700 H -0.16867600 0.23892000 1.05385200 I 2.08454800 -0.56758400 -0.10239100 C -0.29479900 1.16323000 -0.92347700 H 0.34858800 2.01538200 -0.65836900 H -0.11302400 0.89358600 -1.97248000 H -1.34769900 1.46142600 -0.81118900 P 5.77785100 -1.27731100 -0.39464200 F 6.68812800 -0.02211400 -0.85067600 F 6.36195800 -2.33484200 -1.46775500 F 6.70243700 -1.73768800 0.84828200

		C	0.00000000	0.00000000	0.00000000
		I	2.13165800	-0.40120100	-0.20596900
		C	-0.34887100	1.00910400	-0.99007300
		N	-0.63832300	1.83891400	-1.74435300
		I	-1.15433400	-1.78670900	-0.45180600
		C	-0.30472400	0.47573800	1.41762100
CN, CH ₃	-1402.90664254	H	-0.03212100	-0.30207100	2.14154800
		H	0.27006700	1.38943600	1.62632500
		H	-1.37845400	0.69539000	1.50323400
		P	5.79754500	-1.03662500	-0.40604500
		F	6.69957000	-0.57336800	-1.66131400
		F	6.34073600	-2.55477000	-0.32603900
		F	6.74733000	-0.42975600	0.75014800
		C	0.00000000	0.00000000	0.00000000
		I	-1.18433600	-1.82494800	-0.00949400
		C	-0.30285600	0.74356400	1.21529500
		N	-0.53620700	1.32425200	2.18828500
		I	2.13903900	-0.42753400	-0.02922100
CN, CN	-1455.8127619	C	-0.32987200	0.77297900	-1.18969600
		N	-0.58498000	1.37698000	-2.14283100
		P	5.73346000	-1.01000300	-0.01593800
		F	6.73011400	0.11072900	-0.60489800
		F	6.38642900	-2.27653000	-0.76967300
		F	6.47470200	-1.21522800	1.40036200
		C	0.00000000	0.00000000	0.00000000
		I	2.12351700	-0.52515200	-0.04841900
		C	-0.32865100	0.80702300	-1.24435300
		H	-0.11595700	0.24781400	-2.16369500
		H	-1.39728600	1.07239800	-1.22787000
		H	0.26842600	1.73239800	-1.24210400
		I	-1.18297300	-1.83545000	-0.01850300
CH ₃ , CH ₃	-1349.98992159	C	-0.28436000	0.75335900	1.28814100
		H	-0.03976800	0.15597000	2.17492600
		H	0.31274000	1.67859700	1.30408900
		H	-1.35277200	1.01819900	1.32056900
		P	5.83463400	-1.25240600	-0.02635500
		F	6.83153400	-0.11440800	-0.59651300
		F	6.52748600	-2.50353200	-0.77937200
		F	6.57515300	-1.45496900	1.39605400

C 0.00000000 0.00000000 0.00000000
 C 0.46728000 -0.73525300 1.25502900
 C 0.07076700 0.00101400 2.53346500
 C -1.42646800 0.32429700 2.56962100
 C -1.85842600 1.09084600 1.31912700
 C -1.49689800 0.32359900 0.04694900
 H -2.07920300 -0.61059300 -0.00634000
 H -1.75436700 0.91194200 -0.84645300
 H -2.94059200 1.28636300 1.34928500
 H -1.35726500 2.07514400 1.30491100
 H -2.00445400 -0.61013400 2.65571700
 H -1.63409100 0.91300900 3.47566300
 H 0.38042600 -0.57351200 3.41722900
 H 0.64277500 0.94614200 2.53806700
 I -0.35641500 -2.76822800 1.27841300
 I 2.64673600 -0.91426800 1.19389200
 H 0.57088000 0.94507500 -0.03757700
 H 0.25991500 -0.57548200 -0.89904400
 P 6.41954100 -1.18956500 1.25833500
 F 7.07309500 -1.80396600 2.60310200
 F 7.35549700 0.12680400 1.18084100
 F 7.26797300 -2.08352100 0.21219400

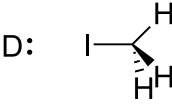
CH₃I	RM062X energy (a. u.)	Cartesian coordinates		
D:		C	0.00000000	0.00000000
	-976.378247691	I	-2.14529100	0.05389000
		H	0.31584000	-0.99229500
		H	0.28899700	0.18451700
		H	-0.37342300	0.78366900
		P	-5.92285600	0.05069000
		F	-6.70109000	0.90808100
		F	-6.84465600	0.50632200
		F	-6.67115900	-1.35428700
				-0.19796500

5.1.3 Ground state, NH₃ as electron donor

(R ₁ , R ₂)	RM062X energy (a. u.)	Cartesian coordinates
H, H	-687.051863526	C 0.00000000 0.00000000 0.00000000 I -1.63207000 -1.39514700 -0.00037400 H -0.10760100 0.60705100 0.90262800 I 1.95319800 -0.88188600 -0.00049700 H -0.10774000 0.60772600 -0.90215700 N 4.75112600 -2.09036000 -0.00027500 H 5.40402800 -1.60428000 -0.61687700 H 4.73550100 -3.06364500 -0.30910600 H 5.17877300 -2.09086300 0.92705600
H, CN	-779.272319394	C 0.00000000 0.00000000 0.00000000 I 2.00425700 -0.70686900 -0.42948200 C -0.21855800 1.30695000 -0.58806400 N -0.37849400 2.35634100 -1.05179300 I -1.55053500 -1.36076100 -0.64309400 H -0.09740600 0.06000500 1.08829900 N 4.70409500 -1.62822800 -1.00066100 H 5.20737200 -0.95121700 -1.57662500 H 4.70956900 -2.50828300 -1.51901800 H 5.27533000 -1.77959300 -0.16767400
H, CH ₃	-726.350611316	C 0.00000000 0.00000000 0.00000000 I 1.55522000 -1.44434400 0.44774900 H 0.09801900 0.16638400 -1.07696000 I -1.97507300 -0.82127300 0.29478000 C 0.20609900 1.26855400 0.80342000 H -0.55956000 2.00644000 0.51880500 H 0.11982600 1.07177200 1.88084100 H 1.20149500 1.68972900 0.59838000 N -4.80279800 -1.94354900 0.71108400 H -4.96091300 -2.22233000 1.68063200 H -4.95937500 -2.77816800 0.14381400 H -5.55151800 -1.29090800 0.47430700

		C	0.00000000	0.00000000	0.00000000
		I	2.02095900	-0.76977100	-0.30069500
		C	-0.20664000	1.09776300	-0.93398700
		N	-0.36288200	1.99860000	-1.64588200
		I	-1.47943300	-1.53122400	-0.47835400
		C	-0.18861300	0.45841400	1.44413200
CN, CH ₃	-818.571199043	H	-0.03198100	-0.38578200	2.12742900
		H	0.54455100	1.24705800	1.66879400
		H	-1.20332800	0.85795300	1.58279000
		N	4.75333900	-1.76923100	-0.67329100
		H	5.20079300	-1.30779500	-1.46709000
		H	4.78083800	-2.77120100	-0.86916400
		H	5.36319400	-1.61518600	0.13124800
		C	0.00000000	0.00000000	0.00000000
		I	-1.47212800	-1.60663500	0.00011200
		C	-0.19070700	0.79901400	1.20136800
		N	-0.31921600	1.42065700	2.16933000
		I	2.05867000	-0.80046200	0.00048600
CN, CN	-871.483391779	C	-0.19026400	0.79846800	-1.20179900
		N	-0.31797900	1.41963200	-2.17017400
		N	4.63577100	-1.78610300	-0.00016900
		H	4.91022700	-2.14440300	-0.91657400
		H	4.76125100	-2.55104100	0.66511700
		H	5.31477700	-1.06474700	0.24915100
		C	0.00000000	0.00000000	0.00000000
		I	1.48179300	-1.61912100	-0.00020600
		C	0.19720900	0.82179800	-1.26352100
		H	0.06441400	0.21669700	-2.16904900
		H	-0.54065200	1.64013700	-1.27391700
		H	1.20948300	1.25570500	-1.26928900
		I	-2.00187200	-0.86168600	-0.00051900
CH ₃ , CH ₃	-765.649439316	C	0.19681300	0.82112500	1.26402700
		H	0.06376300	0.21551900	2.16917900
		H	1.20907300	1.25505700	1.27033500
		H	-0.54107700	1.63943500	1.27465100
		N	-4.84766300	-2.05576900	0.00018400
		H	-5.56092400	-1.46199300	-0.42543000
		H	-5.17614200	-2.26875600	0.94323100
		H	-4.86309400	-2.93743000	-0.51471900

C 0.00000000 0.00000000 0.00000000
 C -0.43967600 -0.73647700 -1.26549300
 C 0.00017500 0.00000900 -2.53092100
 C 1.49272500 0.34211000 -2.52720400
 C 1.88068900 1.11394200 -1.26532100
 C 1.49255200 0.34208600 -0.00350800
 H 2.08422600 -0.58547400 0.06402300
 H 1.72110000 0.93344300 0.89615700
 H 2.96085800 1.32408700 -1.26524300
 H 1.36598900 2.09166500 -1.26534700
 H 2.08441400 -0.58544400 -2.59467200
 H 1.72139300 0.93348400 -3.42682600
 H -0.27839000 -0.57771600 -3.42330000
 H -0.58290200 0.93877000 -2.55594300
 I 0.42758100 -2.76344400 -1.26543300
 I -2.60838600 -0.94742700 -1.26563300
 H -0.58308200 0.93876000 0.02496300
 H -0.27868500 -0.57774400 0.89232900
 N -5.68808500 -1.21557400 -1.26512400
 H -6.15298300 -0.67282100 -1.99432900
 H -6.11711500 -0.93657900 -0.38160800
 H -5.95436100 -2.18939100 -1.41834600

CH₃I	RM062X energy (a. u.)	Cartesian coordinates		
D:		-392.03636378	C 0.00000000 0.00000000 0.00000000	
			I -2.15160000 -0.00113100 0.00474200	
			H 0.33787000 -0.92359800 -0.47975500	
			H 0.33647700 0.87700300 -0.56121800	
			H 0.34051500 0.04732100 1.03880600	
			N -5.29733400 -0.00043400 0.00207700	
			H -5.67901000 0.01927900 -0.94468600	
			H -5.69051500 0.80762700 0.48672500	
			H -5.69268500 -0.82640200 0.45363000	

5.1.4 Ground state, no XB

(R₁, R₂)	RM062X energy (a. u.)	Cartesian coordinates
H, H	-630.512241121	C 0.00000000 0.00000000 0.00000000 I -1.80438000 -1.14881400 -0.00001400 H -0.00003700 0.61146700 0.90504200 I 1.80430700 -1.14881800 -0.00004600 H 0.00002500 0.61146000 -0.90504600
H, CN	-722.728477349	C 0.00000000 0.00000000 0.00000000 I 1.80348300 -1.00548600 -0.61487000 C -0.00006600 1.36894000 -0.47857200 N -0.00224300 2.46591500 -0.84878200 I -1.80338100 -1.00602600 -0.61482700 H 0.00001000 -0.01747300 1.09395300
H, CH ₃	-669.811815246	C 0.00000000 0.00000000 0.00000000 I -1.78920100 -1.10468400 -0.49614100 H 0.00005500 0.05151200 1.09232500 I 1.78928200 -1.10468300 -0.49614000 C 0.00004400 1.36461600 -0.65667400 H 0.89580100 1.92182800 -0.34462600 H 0.00006600 1.27687900 -1.75141400 H -0.89573500 1.92183500 -0.34468200

CN, CH ₃	-762.028363575	C 0.00000000 0.00000000 0.00000000
		I 1.78708200 -1.13176700 -0.50914400
		C 0.00000100 1.20547200 -0.81705200
		N -0.00048700 2.18893600 -1.42867500
		I -1.78703700 -1.13187900 -0.50910500
		C 0.00002700 0.33367200 1.48890300
		H 0.00011700 -0.58995800 2.08050200
		H 0.89662200 0.92294500 1.72881500
		H -0.89666200 0.92278300 1.72889100

CN, CN	-814.934706235	C 0.00000000 0.00000000 0.00000000
		I -1.79971600 -1.22431500 -0.00018600
		C -0.00011900 0.82290700 1.20219500
		N -0.00143600 1.46554200 2.16416700
		I 1.79972300 -1.22429700 0.00027200
		C 0.00008000 0.82256200 -1.20247300
		N 0.00135600 1.46490600 -2.16464100

CH ₃ , CH ₃	-709.111183247	C 0.00000000 0.00000000 0.00000000
		I 1.77899100 -1.26899700 -0.00002300
		C -0.00003100 0.83882900 -1.26675100
		H -0.00026500 0.21610400 -2.16968900
		H -0.89609400 1.47897400 -1.27391200
		H 0.89627600 1.47863300 -1.27414400
		I -1.77900900 -1.26899900 0.00000900
		C -0.00000700 0.83881500 1.26676100
		H -0.00021300 0.21607900 2.16969100
		H 0.89629400 1.47862700 1.27414000
		H -0.89607500 1.47895100 1.27395000

C 0.00000000 0.00000000 0.00000000
C -0.42302000 -0.74142900 -1.26715600
C -0.00003100 0.00017800 -2.53422300
C 1.49255200 0.34612600 -2.52897600
C 1.87786600 1.11864900 -1.26704000
C 1.49259000 0.34589700 -0.00523600
H 2.08726000 -0.57944300 0.06476600
H 1.71653600 0.93813900 0.89470700
H 2.95738000 1.33106900 -1.26703300
H 1.36148200 2.09529800 -1.26694400
H 2.08724800 -0.57918100 -2.59917800
H 1.71645000 0.93854500 -3.42881500
H -0.27673700 -0.57880500 -3.42592900
H -0.58589600 0.93650500 -2.55559600
I 0.43353500 -2.76262100 -1.26729600
I -2.59853900 -0.95192800 -1.26714100
H -0.58583800 0.93634000 0.02151200
H -0.27670000 -0.57909700 0.89163400

5.2 Transition state

5.2.1 Transition state, CO as electron donor

(R ₁ , R ₂)	RM062X energy (a. u.)	Cartesian coordinates
H, H	-1039.51712419	C 0.00000000 0.00000000 0.00000000 I 2.65613200 -0.58292600 -0.00219600 H -0.00007100 -0.50628600 0.95686800 I 0.00071700 2.09505600 0.00738500 H 0.00002300 -0.49944600 -0.96046000 I -2.65643000 -0.58111200 -0.00219700 C 0.00234500 5.54459200 0.00004200 O 0.00243800 6.67363800 -0.01763800
H, CN	-1131.73817019	C 0.00000000 0.00000000 0.00000000 I 2.69842900 -0.43353700 -0.34879400 C 0.00058000 -0.67576000 1.26411500 N 0.00096000 -1.16722300 2.31561500 I -0.00101700 2.10805500 0.01236900 H 0.00024600 -0.52188000 -0.94593700 C -0.00250700 5.45351400 -0.02897300 O -0.00454100 6.58179900 -0.05848100 I -2.69703400 -0.43677000 -0.34883400
H, CH ₃	-1078.81127247	C 0.00000000 0.00000000 0.00000000 I 0.00851600 2.09746800 -0.14803800 H -0.00231500 -0.53244700 -0.94157700 I 2.72182500 -0.55619900 -0.49238900 C -0.00268900 -0.59800400 1.37799800 H -0.00808800 -1.69275300 1.29065700 H 0.89680600 -0.27816100 1.92009800 H -0.89875000 -0.26934700 1.92051300 I -2.72700600 -0.53288700 -0.49249500 C 0.01743400 5.56597800 -0.41618800 O 0.03867100 6.68800500 -0.54136100

		C	0.00000000	0.00000000	0.00000000
		I	0.00003800	2.12215000	0.08710800
		C	-0.00001100	-0.70556000	1.25415500
		N	-0.00001900	-1.26343500	2.27327900
		I	-2.85470500	-0.25236900	0.15943800
CN, CH ₃	-1171.02436666	C	-0.00002100	-0.65604800	-1.37081300
		H	-0.89701600	-0.35508700	-1.92150000
		H	0.89701300	-0.35518200	-1.92148900
		H	-0.00008200	-1.74634200	-1.23967000
		I	2.85469600	-0.25246700	0.15943600
		C	0.00014000	5.47569300	0.31550000
		O	0.00015000	6.57854700	0.55614800
		C	0.00000000	0.00000000	0.00000000
		I	-2.78634000	-0.21332600	-0.00035200
		C	-0.00454000	-0.68778400	-1.26245000
		N	-0.00742600	-1.19646100	-2.30494300
CN, CN	-1223.94844478	I	0.01366400	2.13317000	0.00420600
		C	-0.00457100	-0.69255500	1.25984400
		N	-0.00752800	-1.20526600	2.30035900
		I	2.78345300	-0.24826200	-0.00034000
		C	0.03921800	5.39993000	0.00644000
		O	0.05619600	6.52794800	-0.00938700
		C	0.00000000	0.00000000	0.00000000
		I	0.05739900	2.08493300	-0.00576800
		C	-0.01869000	-0.67253200	-1.33628800
		H	0.88615700	-0.39452300	-1.89024300
		H	-0.04955800	-1.76065500	-1.19650400
		H	-0.90621700	-0.34388200	-1.89051600
		I	3.16292100	-0.41961700	0.00104100
CH ₃ , CH ₃	-1118.09630989	C	-0.01826500	-0.66535700	1.33989300
		H	0.88647300	-0.38405200	1.89234000
		H	-0.90599800	-0.33415700	1.89226400
		H	-0.04870000	-1.75422400	1.20589800
		I	-3.18142100	-0.25329000	0.00114100
		C	0.22884100	5.53683800	-0.00337000
		O	0.33345300	6.66049500	0.01236900

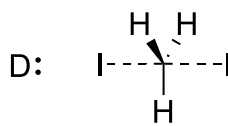
		C	0.00000000	0.00000000	0.00000000
		C	-0.00071500	0.68033400	-1.32906300
		C	0.00009600	-0.00143500	-2.65741000
		C	-0.04380000	-1.53356000	-2.57890700
		C	0.63695100	-2.08796700	-1.32766200
		C	-0.04321400	-1.53225200	-0.07666000
		H	-1.10203900	-1.83740100	-0.07870600
		H	0.42769600	-1.93486300	0.83251600
		H	0.55350000	-3.18611000	-1.32704300
		H	1.70732100	-1.83043600	-1.32804400
@Cy	-1234.7966721	H	-1.10281000	-1.83806800	-2.57569300
		H	0.42621300	-1.93753000	-3.48794300
		H	-0.87318400	0.38720600	-3.20445500
		H	0.89676100	0.35911600	-3.18251700
		I	-3.33466200	0.01932200	-1.32882100
		I	-0.29194500	2.74036800	-1.33012700
		H	0.89656200	0.36149500	0.52464100
		H	-0.87332600	0.38905600	0.54668300
		C	-1.17016200	6.06321800	-1.32740600
		O	-1.66525100	7.07733100	-1.32635000
		I	3.16436400	0.87339600	-1.32873900

5.2.2 Transition state, PF₃ as electron donor

(R ₁ , R ₂)	RM062X energy (a. u.)	Cartesian coordinates		
H, H	-1567.10426806	C	0.00000000	0.00000000
		I	0.73777000	2.60540200
		H	0.51708500	-0.03711700
		I	-2.09213900	0.14942800
		H	0.47388700	-0.03380800
		I	0.35822900	-2.68449200
		P	-5.76277500	0.22095600
		F	-6.68960500	1.46199500
		F	-6.57629400	-0.92291100
		F	-6.51199500	-0.00675100
				-1.41787400
H, CN	-1659.32425434	C	0.00000000	0.00000000
		I	0.27025200	2.71019100
		C	0.71032900	0.03605100
		N	1.23303000	0.06262800
		I	-2.10487400	-0.10556700
		H	0.48409600	0.02452500
		I	0.54284900	-2.66852700
		P	-5.74155100	-0.15398600
		F	-6.52228500	1.24956700
		F	-6.71064200	-0.72250500
		F	-6.46335600	-0.93629700
				-1.25158400
H, CH ₃	-1606.39847106	C	0.00000000	0.00000000
		I	-2.09525000	-0.16731900
		H	0.52792500	0.04371600
		I	0.29794800	2.74614700
		C	0.58367800	0.04546500
		H	0.33355400	-0.87809800
		H	1.67512400	0.13699100
		H	0.18395800	0.91180400
		I	0.73184900	-2.66268600
		P	-5.78148100	-0.24923100
		F	-6.56393700	0.03360400
		F	-6.58534700	0.85135500
		F	-6.68861900	-1.51738100
				0.11488600

CN, CH ₃	-1698.61079703	C	0.00000000	0.00000000	0.00000000
		I	-2.10531900	-0.17393300	0.24667300
		C	0.78967300	0.06650400	1.20007800
		N	1.41877700	0.11944800	2.17537800
		I	0.48524300	-2.81223900	0.14635800
		C	0.54400500	0.04459500	-1.41860400
		H	0.27975200	-0.87821700	-1.94482700
		H	0.13030700	0.91036300	-1.94539800
		H	1.63727700	0.13619400	-1.36857600
		I	0.01272800	2.85353500	0.14281700
		P	-5.74376800	-0.28672400	0.29108500
		F	-6.53325400	1.11278700	0.08992600
		F	-6.72075600	-0.87145700	1.44566400
		F	-6.45044300	-1.06375900	-0.94282200
		C	0.00000000	0.00000000	0.00000000
CN, CN	-1751.5337489	I	-0.11873800	2.78777500	0.00589800
		C	0.64190200	0.07960600	1.28267200
		N	1.11753700	0.13804000	2.33897800
		I	-2.11636800	-0.25701600	-0.06437800
		C	0.71831700	0.08856800	-1.24083600
		N	1.25677000	0.15438000	-2.26610000
		I	0.55537900	-2.73172800	0.00684300
		P	-5.69360400	-0.40438200	-0.01891800
		F	-6.54538500	0.47941500	-1.07383400
		F	-6.38570200	0.19151600	1.31634100
		F	-6.61614700	-1.73221000	-0.11808600
		C	0.00000000	0.00000000	0.00000000
		I	-2.09301700	0.15956100	0.04758500
		C	0.63029100	-0.05121400	-1.36245500
		H	0.39589200	0.86953000	-1.90844700
CH ₃ , CH ₃	-1645.68231895	H	1.71827900	-0.14579600	-1.24796500
		H	0.24218200	-0.91576100	-1.91262300
		I	0.52082200	3.07476500	-0.00740200
		C	0.69080400	-0.05219200	1.33279100
		H	0.47200500	0.86324600	1.89387300
		H	0.33578100	-0.92335800	1.89487200
		H	1.77354000	-0.13487500	1.16970700
		I	0.05280200	-3.11925300	-0.00675900
		P	-5.80723100	0.31719200	0.00908900
		F	-6.69044600	-0.68704000	0.92389100
		F	-6.56681000	-0.00114500	-1.38600500
		F	-6.64929900	1.65634700	0.36212500

		C 0.00000000 0.00000000 0.00000000
		C -0.75188500 -0.12983500 1.28734400
		C -0.17515100 -0.00935500 2.66293800
		C 1.31729900 0.34943300 2.67940000
		C 2.07838200 -0.20274500 1.47428300
		C 1.48255200 0.35492600 0.18173000
		H 1.56560300 1.45357300 0.19399200
		H 2.03387000 -0.02023900 -0.69334400
		H 3.13511800 0.09924200 1.54471500
		H 2.04209800 -1.30312200 1.46965400
		H 1.39870800 1.44827200 2.68232800
@Cy	-1762.38244042	H 1.74945600 -0.02809700 3.61811200
		H -0.76641500 0.75527100 3.18880200
		H -0.36903200 -0.96971300 3.16127600
		I -0.81611900 3.19546300 1.29381200
		I -2.83260000 -0.25924900 1.15087400
		H -0.12955300 -0.95499800 -0.52855500
		H -0.51624000 0.77139300 -0.59106000
		I -0.34529800 -3.24673900 1.30136000
		P -6.55265100 -0.27051400 1.30060200
		F -7.12478200 -0.18945300 2.81277100
		F -7.46589700 -1.52623800 0.83472000
		F -7.51488000 0.87819700 0.68504000

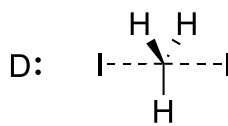
CH₃I	RM062X energy (a. u.)	Cartesian coordinates
D: 	N/A	P 0.00000000 0.00000000 0.00000000 F -1.66879900 -0.01599100 0.11597100 F 0.02167000 -1.28381000 -1.00610700 F -0.02836100 1.15437800 -1.14525900 C 6.97908900 0.00083900 -0.27422300 H 6.66506900 -1.03652900 -0.40401800 H 6.69384600 0.39549100 0.70255100 H 6.63647900 0.63687900 -1.09218000 I 9.15262300 0.00300000 -0.34190000 I 3.17106100 0.09195400 -0.15962500

5.2.3 Transition state, NH₃ as electron donor

(R ₁ , R ₂)	RM062X energy (a. u.)	Cartesian coordinates		
H, H	-982.755292666	C	0.00000000	0.00000000
		I	-2.66850700	-0.58171600
		H	-0.00177700	-0.51958200
		I	0.00629900	2.09808900
		H	-0.00173700	-0.50986200
		I	2.66457000	-0.59737900
		N	0.02883500	5.23666300
		H	-0.81293800	5.60796400
		H	0.09474000	5.66101700
		H	0.82532000	5.57369300
				0.56491100
H, CN	-1074.97854623	C	0.00000000	0.00000000
		I	2.70528700	-0.44139300
		C	0.00070200	-0.67028100
		N	0.00111500	-1.15154600
		I	-0.00194100	2.11658900
		H	0.00073000	-0.54460700
		I	-2.70417500	-0.44630200
		N	-0.00954000	5.13339400
		H	-0.93101500	5.50586400
		H	0.24997500	5.51593400
		H	0.64744800	5.51270200
H, CH ₃	-1022.05608145	C	0.00000000	0.00000000
		I	-0.12908700	1.97329500
		H	0.15489300	-0.75494700
		I	2.79991800	-0.39011400
		C	-0.09056500	-0.19825300
		H	-0.00449300	-1.27079400
		H	0.72486000	0.34469300
		H	-1.05760100	0.17584600
		I	-2.58597400	-0.93055300
		N	-3.21547500	2.14588300
		H	-2.29742600	2.57091200
		H	-3.35168200	1.54153500
		H	-3.09638100	1.49738500
				2.57708400

CN, CH ₃	-1114.26445132	C	0.00000000	0.00000000	0.00000000
		I	-0.00502800	2.12142100	0.17300900
		C	0.00228500	-0.76410300	1.22049500
		N	0.00366700	-1.36339200	2.21600800
		I	-2.87307500	-0.27312000	0.14616500
		C	0.00163600	-0.61087700	-1.39090300
		H	-0.89487300	-0.28813500	-1.93044700
		H	0.89763600	-0.28546400	-1.92966600
		H	0.00320400	-1.70554900	-1.30561000
		I	2.87533600	-0.25910200	0.14654000
		N	-0.03114300	5.13583100	0.47798700
		H	0.46659600	5.35417500	1.34151400
		H	-0.98616700	5.47757700	0.58792300
		H	0.40237900	5.68565400	-0.26382800
CN, CN	-1167.19090178	C	0.00000000	0.00000000	0.00000000
		I	2.79134800	-0.22730600	0.00012900
		C	0.00029500	-0.69894600	1.25783400
		N	0.00041500	-1.21005700	2.29937800
		I	-0.00038900	2.14957700	-0.00011900
		C	0.00031100	-0.69908500	-1.25775200
		N	0.00042500	-1.21032000	-2.29923600
		I	-2.79087900	-0.22838600	0.00012700
		N	-0.00218900	5.06106000	0.00056100
		H	0.23949300	5.43728200	-0.91655100
		H	0.67264800	5.43765200	0.66673300
		H	-0.91679900	5.43841000	0.24979200
		C	0.00000000	0.00000000	0.00000000
CH ₃ , CH ₃	-1061.33668151	I	0.03151300	2.07753900	-0.00425400
		C	-0.01094300	-0.68464100	-1.32181100
		H	0.88909100	-0.38756600	-1.87661800
		H	-0.02497000	-1.77283300	-1.18449500
		H	-0.90554200	-0.36442400	-1.87270100
		I	3.25708100	-0.39142800	0.00149900
		C	-0.01132700	-0.67924700	1.32461500
		H	0.88984700	-0.38166200	1.87732700
		H	-0.90477900	-0.35524900	1.87508800
		H	-0.02743400	-1.76795500	1.19166000
		I	-3.27257800	-0.31418700	0.00152300
		N	0.19901400	5.14925900	0.00786900
		H	-0.49587900	5.60235300	0.60210100
		H	0.10944400	5.56316800	-0.92047300
		H	1.11677800	5.41833500	0.36425500

		C	0.00000000	0.00000000	0.00000000
		C	0.02944000	0.71949900	1.30408900
		C	0.03043500	0.07379700	2.64664500
		C	0.06969600	-1.45953900	2.61436000
		C	-0.62841700	-2.04587400	1.38815700
		C	0.04325700	-1.52906700	0.11678300
		H	1.10153500	-1.83651900	0.11731600
		H	-0.43551200	-1.95455600	-0.77752400
		H	-0.55369500	-3.14405900	1.41801900
		H	-1.69644400	-1.77798300	1.39200300
		H	1.12750300	-1.76850000	2.60887600
@Cy	-1178.04132367	H	-0.39050200	-1.83355800	3.54084000
		H	0.90188900	0.47953500	3.18492900
		H	-0.86900100	0.45323500	3.15584900
		I	3.39793400	0.05917900	1.28940600
		I	0.34440400	2.76191200	1.24205000
		H	-0.91288300	0.34904300	-0.50718600
		H	0.85608200	0.37664400	-0.58232100
		I	-3.20153500	0.91161400	1.33948200
		N	3.59908600	3.93164300	1.54444900
		H	4.57382000	4.21071800	1.41530100
		H	3.53101300	2.99869100	1.11946000
		H	3.50638800	3.74175200	2.54526000

CH ₃ I	RM062X energy (a. u.)	Cartesian coordinates		
D: 	N/A	N	0.00000000	0.00000000
		H	0.38093500	-0.94491600
		H	0.39543000	0.42329000
		H	0.37964900	0.51595300
		C	-5.55177400	-0.02810900
		H	-5.91199500	0.74996900
		H	-5.85503900	-1.01941500
		H	-5.89143500	0.15671200
		I	-9.08834000	0.02552200
		I	-3.37391000	0.03830500

5.2.4 Transition state, no XB

(R₁, R₂)	RM062X energy (a. u.)	Cartesian coordinates
H, H	-926.221542816	C 0.00000000 0.00000000 0.00000000 I 2.65237700 -0.59021900 -0.00030000 H -0.00016400 -0.49721200 0.96135000 I 0.00025600 2.09467800 -0.00029000 H -0.00030800 -0.49751000 -0.96117400 I -2.65261700 -0.58996300 -0.00029900
H, CN	-1018.44191951	C 0.00000000 0.00000000 0.00000000 I 2.69441300 -0.44397200 -0.35393300 C 0.00006400 -0.67962300 1.26127700 N -0.00001800 -1.17515100 2.31082900 I -0.00011500 2.10575100 0.02859100 H 0.00057800 -0.50941700 -0.95232400 I -2.69435100 -0.44407200 -0.35394500
H, CH ₃	-965.515809431	C 0.00000000 0.00000000 0.00000000 I -0.00027900 2.07986400 -0.30826100 H 0.00056100 -0.59804900 -0.90119900 I 2.72223200 -0.58758900 -0.44805300 C 0.00081100 -0.48661600 1.42067500 H 0.89688800 -0.11749800 1.93633800 H -0.89932400 -0.12539800 1.93483100 H 0.00576100 -1.58492700 1.41729400 I -2.72118400 -0.58814300 -0.44801600

CN, CH ₃	-1057.72824083	C 0.00000000 0.00000000 0.00000000
		I 0.00029800 2.09496800 0.34202800
		C -0.00108100 -0.84635500 1.16286200
		N -0.00132700 -1.51889900 2.11026200
		I -2.85468000 -0.27891500 0.12581500
		C -0.00406900 -0.47976000 -1.44177100
		H -0.89603400 -0.10219300 -1.95191200
		H 0.89830000 -0.12566700 -1.95024000
		H -0.01911000 -1.57796600 -1.44432000
		I 2.85117500 -0.28023200 0.12540200

CN, CN	-1110.65152212	C 0.00000000 0.00000000 0.00000000
		I -2.78473900 -0.23865300 0.00016400
		C -0.00046300 -0.68651400 -1.26240200
		N -0.00107500 -1.19911700 -2.30294900
		I -0.00066600 2.12965800 0.00014500
		C -0.00012100 -0.68673300 1.26229400
		N -0.00071300 -1.19954800 2.30273700
		I 2.78385900 -0.23855400 0.00010700

CH ₃ , CH ₃	-1004.80051206	C 0.00000000 0.00000000 0.00000000
		I -0.00017500 2.08757300 0.00011300
		C -0.00009800 -0.66410800 1.34214800
		H -0.89605100 -0.35862700 1.89532900
		H -0.00120700 -1.75327700 1.20558900
		H 0.89772400 -0.36042300 1.89338400
		I -3.15638000 -0.34788700 0.00006500
		C 0.00152400 -0.66396600 -1.34219700
		H -0.89854300 -0.36490700 -1.89232000
		H 0.89510900 -0.35372300 -1.89657900
		H 0.00869500 -1.75312600 -1.20577600
		I 3.15780100 -0.34739700 0.00019000

		C	0.00000000	0.00000000	0.00000000
		C	-0.09281500	-0.67169400	-1.33023300
		C	0.00011200	0.00010100	-2.66038600
		C	0.25492600	1.51197200	-2.58184300
		C	-0.33837400	2.15742100	-1.32962600
		C	0.25698000	1.51140600	-0.07871500
		H	1.34817400	1.66429300	-0.08135000
		H	-0.15242700	1.97619500	0.83056800
		H	-0.09829900	3.23227200	-1.32966700
@Cy	-1121.50075921	H	-1.43444800	2.05645700	-1.32873600
		H	1.34588900	1.66661900	-2.58168100
		H	-0.15713800	1.97636000	-3.49013100
		H	0.81344500	-0.50380800	-3.20530800
		H	-0.93679000	-0.23459600	-3.18614500
		I	3.28777600	-0.48515200	-1.33067900
		I	-0.10259700	-2.75268800	-1.33040800
		H	-0.93831900	-0.23282000	0.52413800
		H	0.81139100	-0.50516300	0.54660400
		I	-3.25131200	-0.40934500	-1.33080600

5.2.5 Transition state, PH₃ as electron donor

(R ₁ , R ₂)	RM062X energy (a. u.)	Cartesian coordinates
H, H	-1269.328861	C 0.00000000 0.00000000 0.00000000 I -2.51942400 1.00444600 -0.10589700 H -0.18081200 -0.28879800 -1.02884100 I 1.14277600 1.74759200 0.33340500 H -0.35359800 -0.54022200 0.86918600 I 1.94811900 -1.89893000 -0.08165600 P 3.48329500 4.49816600 -0.30009000 H 2.51310300 4.96175500 -1.23626400 H 4.18872700 3.71000300 -1.25505500 H 4.35793100 5.62763000 -0.37544100
H, CN	-1361.55023381	C 0.00000000 0.00000000 0.00000000 I 2.55686700 0.97367900 -0.33683700 C 0.31094500 -0.53615100 1.29279700 N 0.53518600 -0.92048600 2.36486200 I -1.06565200 1.82085800 -0.08026500 H 0.29116500 -0.48742800 -0.91910000 I -2.10320000 -1.74842600 -0.34056000 P -3.06364700 4.77743900 -0.00591100 H -3.68553500 4.94815100 1.26594300 H -4.28295300 4.93938400 -0.72876800 H -2.70062200 6.15178900 -0.13461900
H, CH ₃	-1308.62462958	C 0.00000000 0.00000000 0.00000000 I -0.86134200 1.87838500 -0.38011100 H 0.28789200 -0.54565200 -0.88847200 I 2.72617200 0.63256500 -0.45639200 C 0.17187000 -0.43742100 1.42388400 H 0.80075600 0.28997200 1.95488300 H -0.80749800 -0.50881200 1.91317800 H 0.66206100 -1.42026100 1.43375800 I -2.22170600 -1.65686800 -0.48274300 P -4.46642700 3.13030700 -0.30345800 H -5.79441800 3.36324600 0.17956900 H -4.17387200 2.30927300 0.82487500 H -4.83332500 1.99319800 -1.08168900

CN, CH ₃	-1400.83653516	C 0.00000000 0.00000000 0.00000000 I 0.69067400 2.00935100 -0.08070100 C -0.19485500 -0.57171700 1.30592100 N -0.34601500 -1.02737400 2.36397700 I -2.78152500 0.71196500 0.20361900 C -0.26282600 -0.71619800 -1.31393800 H -1.03088100 -0.17765300 -1.87804800 H 0.66406700 -0.76750600 -1.89455900 H -0.61545200 -1.73321800 -1.09607200 I 2.61504700 -1.15213300 0.16547800 P 2.51084600 5.04477500 0.49360700 H 2.66745200 6.42412900 0.83232500 H 3.88343500 4.90333800 0.13134000 H 2.73353300 4.55287600 1.81236300
CN, CN	-1453.76109417	C 0.00000000 0.00000000 0.00000000 I -2.78646200 -0.21854600 -0.00407700 C -0.00228400 -0.66834100 -1.27292900 N -0.00248900 -1.16152200 -2.32293500 I 0.00639000 2.13990000 0.03838500 C -0.00237900 -0.71622200 1.24661500 N -0.00224800 -1.24939700 2.27688700 I 2.78591500 -0.23528800 -0.00412400 P 0.01918800 5.60626100 -0.01752500 H 0.84371500 6.41170000 0.82169400 H -1.14623900 6.40271400 0.18487500 H 0.39882200 6.27868600 -1.21573400
CH ₃ , CH ₃	-1347.91141116	C 0.00000000 0.00000000 0.00000000 I -0.52709600 2.01843500 -0.03038600 C 0.27475200 -0.60886900 1.34282700 H -0.68315900 -0.72929100 1.86172300 H 0.75456400 -1.58724500 1.21132300 H 0.94819500 0.04219000 1.91534700 I -2.86938700 -1.02606600 -0.02648800 C 0.18504600 -0.67065900 -1.32087800 H -0.61187300 -0.35608300 -1.99962100 H 1.16518600 -0.37825800 -1.72736700 H 0.14594900 -1.75723700 -1.17312800 I 3.23724600 0.53783800 -0.03282800 P -3.94324700 3.36208200 -0.02816900 H -3.85847300 2.18392800 -0.82701700 H -5.33294300 3.60381800 -0.28179900 H -4.10610900 2.68619600 1.21951900

		C	0.00000000	0.00000000	0.00000000
		C	0.14115600	0.66429400	-1.32819900
		C	-0.00051800	-0.00639800	-2.65313500
		C	-0.34825100	-1.49908400	-2.57367500
		C	0.20754600	-2.17700600	-1.32151600
		C	-0.34725600	-1.49319900	-0.07210100
		H	-1.44568700	-1.58082700	-0.07402800
		H	0.03371700	-1.97930000	0.83841000
		H	-0.09541200	-3.23584000	-1.31887700
		H	1.30783500	-2.14056200	-1.32204900
		H	-1.44670900	-1.58633500	-2.57028700
@Cy	-1464.60869905	H	0.03170500	-1.98961700	-3.48223200
		H	-0.78324000	0.54862200	-3.19452900
		H	0.94621700	0.17096800	-3.18448000
		I	-3.27976400	0.67683800	-1.32731300
		I	0.28080400	2.74179100	-1.33338700
		H	0.94675800	0.18029600	0.53028900
		H	-0.78285200	0.55734100	0.53882000
		I	3.28392100	0.20839400	-1.32723500
		P	0.50886600	6.38304700	-1.32182900
		H	-0.57195000	7.23612000	-1.69438900
		H	1.46784200	7.09548300	-2.10164500
		H	0.79854500	7.10988500	-0.12890200

5.3 Electron donors

Electron donor	RM062X energy (a. u.)	Cartesian coordinates
CO	-113.292077853	C 0.00000000 0.00000000 0.00000000 O 0.00000000 0.00000000 1.10206000
PF ₃	-640.876895607	P 0.00000000 0.00000000 0.00000000 F 0.00000000 1.39458200 -0.81937600 F -1.20774300 -0.69729100 -0.81937600 F 1.20774300 -0.69729100 -0.81937600
NH ₃	-56.53057465	N 0.00000000 0.00000000 0.00000000 H 0.00000000 0.94336100 -0.38890600 H -0.81697400 -0.47168000 -0.38890600 H 0.81697400 -0.47168000 -0.38890600
PH ₃	-343.105127268	P 0.00000000 0.00000000 0.00000000 H 0.00000000 1.19829400 -0.77449700 H -1.03775300 -0.59914700 -0.77449700 H 1.03775300 -0.59914700 -0.77449700